

Interactive comment on “Iodine chemistry after dark” by Alfonso Saiz-Lopez et al.

We thank Dr. Louis for the insightful comments. Below we provide a detailed point-by-point answer (AC – Author Comment) to each comment on our manuscript (RC – Referee Comment).

RC:

This paper presents a very interesting study on the iodine atmospheric chemistry using two modelling approaches: one at the molecular level, one at the global level. The potential energy surfaces for three different reactions were explored for the first time by theoretical calculations: $\text{HOI} + \text{NO}_2$, $\text{HOI} + \text{HNO}_3$, and $\text{HOI} + \text{NO}_3$. I have several comments concerning this work. 1) Spin-orbit correction (SOC) is very important for iodine-containing species. The authors stated on page 6 line 12 that "spin-orbit splittings of -17 and -5 kJ mol⁻¹ were applied to energies of I and IO". These values do not correspond to the well-known value for I atom (-30.3 kJ mol⁻¹ from C.E. Moore, Atomic Energy Levels, USGPO, Vols. II and III, NSRDS-NBS 35, Washington, DC, 1971). Over the last years, my group performed theoretical calculations to get the SOC values for numerous iodine-containing species using the CASPT2/RASSI methodology. The corresponding values for I, IO, and HOI are -30.0, -14.4, and -5.9 kJ/mol (Meciarova et al., CPL, 2011, 517, 149; Khanniche et al., JPCA, 2016, 120, 1737; Sulkova et al., JPCA, 2013, 117, 771). These calculations were also validated by comparison to few available data. I recommend the authors to update their energetics according to the correct SOC values. 2) In Table 2, there are several low frequency modes for molecular complexes and transition state. Are they among them one or several which should be treated as hindered rotors? It is also interesting to compare calculated vibrational frequencies for HOI, NO₃, IO, HNO₃ with their available experimental counterparts. 3) Nitrogen oxides also exhibits often an instability of the wavefunction (internal or RHF -> UHF). Is-it the case here for all stationary points? This instability will affect the energetics. The Gaussian09 software includes an option to check it. 4) What is the level of theory used for the energetics? It is not clear.

AC:

Response to Comment 1: the sentence on page 6 should have read spin-orbit “corrections” rather than “splittings”. The sentence has now been rephrased to make this clear.

Response to Comment 2: we not treat the low frequency modes in the HOI-NO₃ and IO-HNO₃ complexes as hindered rotors. In our experience, this level of sophistication in RRKM calculations is only warranted if experimental rate coefficients are available, to which hindered rotor barrier heights can be fitted (ab initio barrier heights are generally not accurate enough).

We have added the following sentence on page 7, line 18 to make these points.

We have previously compared the calculated vibrational frequencies of iodine-containing molecules with available experimental data [Plane et al., 2006], and found this level of theory to be good enough for the purpose of this study.

Response to Comment 3: the nitrogen oxides of relevance to this study are HNO_3 (which does not exhibit an RHF \rightarrow UHF instability at the level of theory used), and NO_2 which is a radical.

Response to Comment 4: the energetics are determined at the same level of theory as the geometry optimisations and vibrational frequency calculations. This is made clearer on page 6.

RC:

Concerning the atmospheric modelling, the reaction of NO_3 with iodocarbons is important as noticed on page 8 line 15, it could be also important to see if adding the reactivity of atmospheric VOC with iodine-containing species will affect the results because this reaction will produce iodocarbons.

AC:

As stated in the referred paragraph, there are many uncertainties about the products of these reactions, and in the case of the $\text{NO}_3 + \text{CH}_2\text{I}_2$ reaction the rate constant is significantly slower than R4. Therefore we have decided not to include these reactions due to the lack of information in the bibliography.

1

Iodine chemistry after dark

2 Alfonso Saiz-Lopez¹, John M.C. Plane², Carlos A. Cuevas¹, Anoop S. Mahajan³, Jean-François
3 Lamarque⁴ and Douglas E. Kinnison⁴

4 ¹Department of Atmospheric Chemistry and Climate, Institute of Physical Chemistry
5 Rocasolano, CSIC, Madrid, Spain

6
7 ²School of Chemistry, University of Leeds, Leeds, UK

8
9 ³Indian Institute of Tropical Meteorology, Pune, India

10
11 ⁴Atmospheric Chemistry Observations and Modelling, NCAR, Colorado, USA

12 Correspondence to: A. Saiz-Lopez (a.saiz@csic.es)

1 **Abstract**

2 Little attention has so far been paid to the nighttime atmospheric chemistry of iodine species.
3 Current atmospheric models predict a buildup of HOI and I₂ during the night that leads to a spike
4 of IO at sunrise, which is not observed by measurements. In this work, electronic structure
5 calculations are used to survey possible reactions that HOI and I₂ could undergo at night in the
6 lower troposphere, and hence reduce their nighttime accumulation. The new reaction NO₃ + HOI
7 → IO + HNO₃ is proposed, with a rate coefficient calculated from statistical rate theory over the
8 temperature range 260 - 300 K and at a pressure of 1000 hPa to be $k(T) = 2.7 \times 10^{-12} (300 \text{ K} / T$
9 $)^{2.66} \text{ cm}^3 \text{ molecule}^{-1} \text{ s}^{-1}$. This reaction is included in two atmospheric models, along with the
10 known reaction between I₂ and NO₃, to explore a new nocturnal iodine radical activation
11 mechanism. The results show that this iodine scheme leads to a considerable reduction of
12 nighttime HOI and I₂, which results in the enhancement of more than 25% of nighttime ocean
13 emissions of HOI + I₂ and the removal of the anomalous spike of IO at sunrise. We suggest that
14 active nighttime iodine can also have a considerable, so far unrecognized, impact on the
15 reduction of the NO₃ radical levels in the [marine boundary layer](#) (MBL) and hence upon the
16 nocturnal oxidizing capacity of the marine atmosphere. The effect of this is exemplified by the
17 indirect effect on dimethyl sulfide (DMS) oxidation.

18

19

20

21

1 **1. Introduction**

2 Active nighttime iodine chemistry was first evidenced a decade ago when it was shown that
3 nocturnal I₂ emitted by macroalgae could react with NO₃ leading to the formation of IO and
4 OIO, which were measured in the coastal MBL at Mace Head, Ireland (Saiz-Lopez and Plane,
5 2004). The nitrate radical has also been recently suggested as a nocturnal loss of CH₂I₂, which
6 helps to reconcile observed and modelled concentrations of this iodocarbon over the remote
7 MBL (Carpenter et al., 2015). However, most of the work on reactive atmospheric iodine has
8 focused on the use of daytime observations and models to assess its role in the catalytic
9 destruction of ozone and the oxidizing capacity of the troposphere (e.g. Saiz-Lopez et al. (2012b)
10 and references therein). In the MBL, iodine-, along with bromine-catalysed ozone destruction
11 contributes up to 45% of the observed daytime depletion (Mahajan et al., 2010a; Read et al.,
12 2008), although this contribution shows large geographical variability (Gómez Martín et al.,
13 2013; Mahajan et al., 2012; Prados-Roman et al., 2015b; Volkamer et al., 2015). Iodine
14 compounds have also been implicated in the formation of aerosols, although the mechanisms and
15 magnitudes of these processes are not fully understood (Allan et al., 2015; Gomez Martin et al.,
16 2013; Hoffmann et al., 2001; McFiggans et al., 2004; O'Dowd et al., 2002; Roscoe et al., 2015).
17 Reactive forms of inorganic iodine may also contribute to the oxidation of elemental mercury
18 over the tropical oceans (Wang et al., 2014). In recent years, iodine sources and chemistry have
19 also been implemented in global models demonstrating the effect of iodine chemistry in the
20 oxidation capacity of the global marine troposphere (Ordóñez et al., 2012; Saiz-Lopez et al.,
21 2012a; Saiz-Lopez et al., 2014; Sherwen et al., 2016).

22 Iodine is emitted into the atmosphere from the ocean surface in both organic and inorganic
23 forms. The main organic compounds emitted are methyl iodide (CH₃I), ethyl iodide (C₂H₅I),

1 propyl iodide (1- and 2-C₃H₇I), chloriodomethane (CH₂ICl), bromiodomethane (CH₂IBr), and
2 diiodomethane (CH₂I₂) (Butler et al., 2007; Carpenter, 2003; Jones et al., 2010; Mahajan et al.,
3 2012). However, these organic compounds contribute only up to a [fourth](#) of the MBL iodine
4 loading (Großmann et al., 2013; Jones et al., 2010; Mahajan et al., 2010a; Prados-Roman et al.,
5 2015b). Inorganic emissions of HOI and I₂, which result from the deposition of O₃ at the ocean
6 surface and subsequent reaction with I⁻ ions in the surface microlayer, account for the main
7 source of iodine in the MBL (Carpenter et al., 2013). Recent laboratory experiments have shown
8 that HOI is the major compound emitted, and provided parameterizations of the fluxes of both
9 species depending on wind speed, temperature, and the concentrations of O₃ and I⁻ (Carpenter et
10 al., 2013; MacDonald et al., 2014). These parameterized fluxes of HOI and I₂ have then been
11 used in a one-dimensional model to study the diurnal evolution of the IO and I₂ mixing ratios at
12 the Cape Verde Atmospheric Observatory (CVAO) (Carpenter et al., 2013; Lawler et al., 2014).
13 The model simulations replicate well the levels and general diurnal profiles of IO and I₂,
14 although an early morning ‘dawn spike’ in IO is predicted by the models, but has not been
15 observed (Mahajan et al., 2010a; Read et al., 2008). The morning peak predicted by current
16 iodine chemistry models is due to a buildup of the emitted I₂ and HOI (which is converted into
17 I₂/IBr/ICl through heterogeneous sea-salt recycling) over the course of the night, followed by
18 rapid photolysis at sunrise.

19 Traditionally it has been thought that iodine chemistry has a negligible effect on oxidizing
20 capacity of the nocturnal marine atmosphere. As a consequence, unlike the demonstrated effect
21 of iodine on the levels of daytime oxidants, the impact of active iodine upon the main nighttime
22 oxidant, NO₃, remains an open question. This is important given that in many parts of the ocean
23 the NO₃ + DMS reaction is at least as important as OH + DMS in oxidizing DMS (Allan et al.,

1 2000), and hence a reduction of NO₃ may have an effect in the production of SO₂ and methane
2 sulfonic acid (MSA). Here, we discuss possible mechanisms of nighttime iodine radical
3 activation and their potential effect on nighttime iodine ocean fluxes and the currently modeled
4 dawn spike in IO. A new reaction of HOI with NO₃ is proposed, supported by theoretical
5 calculations. We explore the implications of this new reaction both for iodine and NO₃
6 chemistries.

7

8 **2. Nocturnal iodine radical activation mechanism**

9 We use the reaction mechanism that has recently been described in a global modelling study by
10 Saiz-Lopez et al. (2014) ([see supplementary information](#)). In addition to the reactions included in
11 that scheme, we also include nighttime gas-phase reactions based on the theoretical calculations
12 described below. The additional reactions are listed in Table 1 and a scheme with this new
13 nocturnal chemistry is included in Figure 1.

14 To the best of our knowledge, reactions of HOI specific to night time have not been studied,
15 either theoretically or through laboratory experiments. Currently, HOI is thought to build up
16 overnight until sunrise, with only heterogeneous uptake on seasalt aerosol as a nighttime loss
17 process (Saiz-Lopez et al., 2012b; Simpson et al., 2015). In addition to the well known I₂ + NO₃
18 reaction (R1) (Chambers et al., 1992), here we consider several possible HOI reactions that could
19 occur at night, in the absence of photolysis and OH:



1 The stationary points on the potential energy surface (PES) for reaction 4 are illustrated in Figure
2 3. HOI and NO₃ associate to form a complex which is 24 kJ mol⁻¹ below the reactant entrance
3 channel. H-atom transfer involves a submerged transition state to form a IO--HNO₃ complex,
4 which can then dissociate to the products IO + HNO₃. Overall, the reaction is exothermic by 11
5 kJ mol⁻¹. The vibrational frequencies, rotational energies and geometries (in Cartesian
6 co-ordinates) of these intermediates are listed in Table 2.

7 The rate coefficient for reaction 4 was then estimated using Rice-Ramsperger-Kassel-Markus
8 (RRKM) theory, employing a multi-well energy-grained master equation solver based on the
9 inverse Laplace transform method - MESMER (Master Equation Solver for Multi-well Energy
10 Reactions) (Roberston et al., 2014). The reaction proceeds via the formation of the excited
11 HOI--NO₃ complex from HOI + NO₃. This complex can then dissociate back to the reactants or
12 rearrange to the IO--HNO₃ intermediate complex over the transition state, which can in turn
13 dissociate to the products IO + HNO₃. Either of the intermediates can also be stabilized by
14 collision with the third body (N₂). The time evolution of all these possible outcomes is modelled
15 using the master equation.

16 The internal energies of the intermediates on the PES were divided into a contiguous set of
17 grains (width 10 cm⁻¹), each containing a bundle of rovibrational states calculated with the
18 molecular parameters in Table 2. It should be noted that the HOI-NO₃ and IO-HNO₃ complexes
19 both have low frequency vibrational modes (< 100 cm⁻¹) which should more correctly be treated
20 as hindered rotors rather than vibrations. However, in our experience this is not worth doing this
21 until experimental rate coefficients are available to fit the rotor barrier heights. In any case, the
22 energies of both complexes are far enough below the energy of the entrance channel (figure 3)
23 that relatively small changes in their densities of states will have a minor effect on the overall

1 [rate coefficient](#). Each grain was then assigned a set of microcanonical rate coefficients linking it
2 to other intermediates, calculated by RRKM theory. For dissociation to products or reactants,
3 microcanonical rate coefficients were determined using inverse Laplace transformation to link
4 them directly to the capture rate coefficient, k_{capture} . For reaction 4 and the reverse reaction IO +
5 HNO₃ involving neutral species, k_{capture} was set to a typical capture rate coefficient of 2.5×10^{-10}
6 $(T/300 \text{ K})^{1/6} \text{ cm}^3 \text{ molecule}^{-1} \text{ s}^{-1}$, where the small positive temperature dependence is
7 characteristic of a long-range potential governed by dispersion and dipole-dipole forces
8 (Georgievskii and Klippenstein, 2005).

9 The probability of collisional transfer between grains was estimated using the exponential down
10 model, where the average energy for downward transitions was set to $\langle \Delta E \rangle_{\text{down}} = 300 \text{ cm}^{-1}$ for
11 N₂ as the third body (Gilbert and Smith, 1990). MESMER determines the temperature- and
12 pressure-dependent rate coefficient from the full microcanonical description of the system time
13 evolution by performing an eigenvector/eigenvalue analysis (Bartis and Widom, 1974). The
14 resulting rate coefficient over the temperature range 260 - 300 K at a pressure of 1000 hPa is
15 $k_4(T) = 2.7 \times 10^{-12} (300 \text{ K} / T)^{2.66} \text{ cm}^3 \text{ molecule}^{-1} \text{ s}^{-1}$. Because the intermediate complexes are
16 not strongly bound, and the transition state and products are below the entrance channel, the only
17 products formed in reaction 4 under atmospheric conditions are IO + HNO₃. The absence of a
18 barrier above the entrance channel, [and the fact that the intermediate complexes and barrier are](#)
19 [well below the entrance channel within their uncertainties](#), means that the uncertainty in k_4
20 principally arises from the estimated capture rate coefficient and so is likely to be no more than a
21 factor of 2.

22 Note that NO₃ also reacts with CH₂I₂ with a rate constant $\sim 2\text{-}4 \times 10^{-13} \text{ cm}^3 \text{ molecule}^{-1} \text{ s}^{-1}$, which
23 can have a significant effect on nighttime CH₂I₂ concentration (Carpenter et al., 2015). However

1 the products of this reaction are still uncertain (Carpenter et al., 2015; Nakano et al., 2006) and
2 its rate is considerably slower than that of R4.

3 In summary, the only likely gas-phase reactions that I₂ and HOI undergo in the nighttime
4 troposphere are R1 and R4, respectively. These are included in the model reaction scheme to
5 examine their impacts on the evolution of iodine species in the atmosphere.

6

7 **4. Atmospheric modelling**

8 We use two atmospheric chemical transport models to study *i*) the impact of this new chemistry
9 on the nighttime chemistry and partitioning of iodine species, and *ii*) the resulting geographical
10 distribution of nocturnal iodine and impact on NO₃ within the global marine boundary layer.

11 The first model, Tropospheric HALogen chemistry MOdel (THAMO), is used for a detailed
12 kinetics study of the impact of the different reactions shown in Table 1 as well as to assess which
13 uptake rates best reproduce observations from a field study at the CVAO (Carpenter et al., 2011).

14 THAMO has been used in the past to study iodine chemistry at the CVAO and further details
15 including the full chemical scheme can be found elsewhere (Lawler et al., 2014; Mahajan et al.,
16 2009; Mahajan et al., 2010a; Mahajan et al., 2010b; Read et al., 2008; Saiz-Lopez et al., 2008).

17 Briefly, THAMO is a 1-D chemistry transport model with 200 stacked boxes at a vertical
18 resolution of 5m (total height 1 km). The model treats iodine, bromine, O₃, NO_x and HO_x
19 chemistry, and is constrained with typical measured values of other chemical species in the
20 MBL: [CO]=110 nmol mol⁻¹; [DMS]=30 pmol/mol; [CH₄]=1820 nmol mol⁻¹; [ethane]=925
21 pmol/mol; [CH₃CHO]=970 pmol/mol; [HCHO]=500 pmol/mol; [isoprene]=10 pmol/mol;
22 [propane]=60 pmol/mol; [propene]=20 pmol/mol. The average background aerosol surface area

1 (ASA) used is $1 \times 10^{-6} \text{ cm}^2 \text{ cm}^{-3}$ (Lee et al., 2009; Lee et al., 2010; Read et al., 2008; Read et al.,
2 2009). The model is initialized at midnight and the evolution of iodine species, O_3 , NO_x and HO_x
3 is followed until the model reaches steady state.

4 The second model is the global 3D chemistry-climate model CAM-Chem (Community
5 Atmospheric Model with chemistry, version 4.0), which is used to study the impact of reactions
6 1 and 4 on a global scale. The model includes a comprehensive chemistry scheme to simulate the
7 evolution of trace gases and aerosols in the troposphere and the stratosphere (Lamarque et al.,
8 2012). The model runs with the iodine and bromine chemistry schemes from previous studies
9 (Fernandez et al., 2014; Saiz-Lopez et al., 2014; Saiz-Lopez et al., 2015), including the
10 photochemical breakdown of bromo- and iodo-carbons emitted from the oceans (Ordóñez et al.,
11 2012) and abiotic oceanic sources of HOI and I_2 (Prados-Roman et al., 2015a). CAM-Chem has
12 been configured in this work with a horizontal resolution of 1.9° latitude by 2.5° longitude and 26
13 vertical levels, from the surface to $\sim 40\text{km}$ altitude. All model runs in this study were performed
14 in the specified dynamics mode (Lamarque et al., 2012) using offline meteorological fields
15 instead of an online calculation, to allow direct comparisons between different simulations. This
16 offline meteorology consists of a high frequency meteorological input from a previous free
17 running climatic simulation.

18 It should be noted that during nighttime the uptake on aerosols of emitted species such as I_2 and
19 HOI, and the uptake of reservoir species such as IONO_2 , can play a major role in the cycling of
20 iodine. Observations at CVAO show that I_2 peaked at about 1 pmol/mol during the night and that
21 ICl was not detected above the 1 pmol/mol detection limit of the instrument (Lawler et al.,
22 2014). In order to match these observations, we need to reduce the uptake and heterogeneous
23 recycling of iodine species. The uptake rates of chemical species on the background seasalt

1 aerosols are determined by their uptake coefficients (γ). The database of mass accommodation
2 and/or uptake coefficients is rather sparse and essentially limited to I_2 , HI, HOI, ICI, IBr on pure
3 water/ice and on sulphuric acid particles (Sander et al., 2006). Other iodine species which are
4 likely to undergo uptake onto aerosol are OIO, HIO₃, INO₂, IONO₂, I₂O₂ (Saiz-Lopez et al.,
5 2012a; Sommariva et al., 2012). Uptake of HOI is very uncertain, with $\gamma(\text{HOI})$ ranging from $2 \times$
6 10^{-3} to 0.3 depending on the surface composition and state (Holmes et al., 2001). Sommariva et
7 al. (2012) assumed $\gamma(\text{HOI})$ to be 0.6, similar to the value for HOBr measured by Wachsmuth et
8 al. (2002). In the case of IONO₂, the uptake coefficient has not been measured, with most models
9 using values of 0.1 (Lawler et al., 2014; Leigh et al., 2010; Mahajan et al., 2009; Mahajan et al.,
10 2010a; Mahajan et al., 2010b; Saiz-Lopez et al., 2008; Sommariva et al., 2012; von Glasow et
11 al., 2002). The modelled levels of I_2 and ICI change with different values of uptake coefficients.
12 To match the CVAO I_2 and ICI observations (Lawler et al., 2014), we have used $\gamma = 0.01$ for
13 HOI and IONO₂, which is within the uncertainty in the literature, and assumed that 80% is
14 recycled as I_2 . Further measurements of these dihalogen species are needed to better constrain
15 their heterogeneous recycling on seasalt aerosols.

16

17 **5. Results and discussion**

18 Of the possible nocturnal iodine activation reactions involving the inorganic iodine source gases
19 I_2 and HOI, only reactions R1 and R4 appear to be likely candidates (see Section 3). We
20 therefore designed two modelling scenarios: Scenario 1 (S1), without nighttime reactions of I_2 or
21 HOI with NO₃; and Scenario 2 (S2), including reactions R1 and R4 for the degradation of HOI
22 and I_2 by NO₃. In the one-dimensional model THAMO, the I_2 and HOI are injected into the

1 atmosphere from the ocean surface using the flux parameterizations derived from laboratory
2 experiments (Carpenter et al., 2013; MacDonald et al., 2014). Figure 4 shows the resulting
3 diurnal evolution of the HOI and I₂ mixing ratios in the two scenarios. The I₂ mixing ratio peaks
4 during the night in both the scenarios due to quick loss by photolysis during the daytime. By
5 contrast, HOI is present during daytime due to its production through the reaction of IO with
6 HO₂, and peaks just before sunset. In the first scenario, without the inclusion of reactions R1 and
7 R4, Figure 4 (right-hand side panels) shows that HOI and I₂ both build up during the night,
8 reaching a concentration peak just before dawn. This is especially noticeable for I₂ as the
9 daytime concentrations are much lower than during the night. For both species, inclusion of
10 reactions with NO₃ causes a decrease in their respective nocturnal concentrations (Fig. 4, left-
11 hand side panels). The inclusion of reactions R1 and R4 also leads to a modelled I₂ concentration
12 which is in better agreement with the observations of the molecule made at CVAO (Lawler et
13 al., 2014), reaching peak values of about 1 pmol/mol, as compared to about 3 pmol/mol for the
14 scenario without nighttime reactions. An additional consequence of including reactions R1 and
15 R4 is the significant increase of the sea-air fluxes of HOI and I₂ at night due to their atmospheric
16 removal by NO₃ (Fig. 4, bottom panel).

17 Figure 5 shows the diurnal evolution of IO, NO₃ and IONO₂ in both model scenarios. Although
18 the daytime peak values of IO are well reproduced in both scenarios, reaching about 1.5
19 pmol/mol around noon similar to the ground-based observations (Read et al., 2008), the inclusion
20 of reactions R1 and R4 leads to the removal of the dawn spike in IO, which is predicted by
21 current iodine models but was not observed at CVAO (Mahajan et al., 2010a; Read et al., 2008) .
22 The IO dawn spike predicted by models is due to a buildup of the emitted I₂ and HOI (which is
23 converted into I₂/IBr/ICl through heterogeneous recycling) over the night, followed by rapid

1 photolysis after first sunlight. However, due to the considerable removal of HOI and I₂ through
2 the night due to reaction with ambient NO₃, this spike does not appear in the second scenario,
3 leading to a modification of the diurnal profile of IO that better matches with observations.

4 Reactions R1 and R4 also reduce the NO₃ mixing ratio (Fig. 5, middle panels). In scenario 1, the
5 NO₃ is modelled to peak at about 14 pmol/mol just before dawn. However, the inclusion of
6 reactions R1 and R4 leads to near complete depletion of NO₃ close to the surface, with the peak
7 level at the surface reaching only 2 pmol/mol, since reactions R1 and R4 become the main
8 atmospheric loss processes for NO₃ in the lower MBL. These reactions lead however to the
9 buildup of IONO₂ during the night (Fig. 5, bottom panels). In the absence of reactions R1 and
10 R4, significant levels of IONO₂ are seen only at dawn and dusk since no other reactions produce
11 IONO₂ at night, and during the day IONO₂ is removed by photolysis. However, with continuous
12 conversion of I₂ and HOI to IONO₂ by reactions R1 and R4 in scenario 2, IONO₂ is modelled to
13 reach up to 3 pmol/mol in the nocturnal MBL.

14 Given the associated uncertainty in the theoretical estimate of the k_4 , we used THAMO to assess
15 the sensitivity of surface NO₃ to k_4 . Figure 6 shows that NO₃ is in fact highly coupled to k_4 , with
16 the expected uncertainty in k_4 of **one order of magnitude** (see above) giving rise to a **factor of two**
17 **change in NO₃**. A laboratory measurement of k_4 should therefore be undertaken in the future.

18 We now implement the nighttime reactions in the 3D global model (CAM-Chem) to assess the
19 resulting geographical distributions and impacts of these reactions. We have also run two
20 different scenarios in CAM-Chem, the first without R1 and R4 in the chemical scheme, and the
21 second including the new nighttime iodine chemistry. Figure 7 shows how the inclusion of R1
22 and R4 reduces globally the nighttime concentrations of I₂ and HOI. The plots correspond to the

1 **nighttime** averaged (from 00LT to 01LT) differences between the model scenarios. Considerable
2 reductions of up to 0.5 and 10 pmol/mol (i.e. up to 100% removal) are observed for I₂ and HOI,
3 respectively, particularly over coastal polluted regions where continental pollution outflow leads
4 to higher levels of NO₃ in the nighttime MBL. Major shipping routes also show strong nocturnal
5 iodine activity due to the characteristically high NO_x, and resulting NO₃, associated with
6 shipping emissions.

7 Figure 8 shows the effect of this nocturnal chemistry on the concentrations of IONO₂ and NO₃.
8 As in the previous figure, the plots correspond to the nighttime averaged difference between the
9 second and the first scenarios. The maps show an increase of IONO₂ of up to 15 pmol/mol
10 (~600%) over polluted coastal areas, due to efficient conversion of NO₃ into IONO₂. The bottom
11 panel of Figure 7 shows the expected decrease of NO₃ levels associated with the inclusion of
12 reactions R1 and R4, with decreases of up to ~4 pmol/mol (up to 60%) over marine polluted
13 regions. We model global percentage reductions in the NO₃ concentrations of 7.1% (60S-60N),
14 with nitrate removal of up to 80% in non-polluted remote oceanic regions with low NO₃ levels.
15 This in turn can affect the modelled oxidation of DMS by NO₃. We estimate that the reduction in
16 NO₃, due to the inclusion of R1 and R4, results in a model increase in DMS levels of up to 7
17 pmol/mol (about 20%) in marine regions affected by continental pollution outflow (Fig. 9). We
18 therefore suggest that the inclusion of the new nighttime iodine chemistry can have a large, so far
19 unrecognized, impact on the nocturnal oxidizing capacity of the marine atmosphere.

20 The hourly evolution of the main species involved in this study is shown in Figures 10 and 11,
21 which include the levels of HOI, I₂, IONO₂ and NO₃ in the MBL over regions where nocturnal
22 iodine is modelled to be particularly active. The first region is located within the Mediterranean
23 Sea, an area that shows large differences during the summer months when high ozone levels

1 drive large emissions of HOI and I₂ from the sea, and the high levels of NO₃ at nighttime make
2 this chemistry especially important. The hourly average in August is shown in Figure 10 for
3 HOI, IONO₂ and I₂. HOI and IONO₂ (Fig 10) are the species whose concentration differ most
4 between scenarios as HOI is removed and IONO₂ produced by R4 (and, to a lesser extent, R1).
5 Over a Pacific Ocean region at the south of the Baja California Peninsula, the modelled
6 differences between the two scenarios are even higher than over the Mediterranean Sea (Figure
7 11). Large differences in MBL NO₃, up to 28%, are modelled during the night caused by
8 pollution outflow from the west coasts of Mexico and USA.

9

10 **6. Summary and conclusions**

11 The viability of the reaction of HOI with NO₂, HNO₃ and NO₃ has been studied by theoretical
12 calculations. The results indicate that only the reaction of HOI with NO₃, to yield IO + HNO₃, is
13 possible under tropospheric conditions. The inclusion of this reaction, along with that of I₂ +
14 NO₃, has a number of significant implications: *i*) nocturnal iodine radical chemistry is activated;
15 *ii*) this causes enhanced nighttime oceanic emissions of HOI and I₂; *iii*) nighttime iodine species
16 are partitioned into high levels of IONO₂; *iv*) the IO spike, modelled by current iodine models
17 but not shown by observations, is removed; and, *v*) a reduction of the levels of nitrate radical in
18 the MBL, with the associated less efficient oxidation of DMS, which has important implications
19 for our understanding of the nocturnal oxidizing capacity of the marine atmosphere.

20

21

1 **Acknowledgments**

2 This work was supported by the Spanish National Research Council (CSIC). The National
3 Center for Atmospheric Research (NCAR) is funded by the National Science Foundation NSF.
4 The Climate Simulation Laboratory at NCAR's Computational and Information Systems
5 Laboratory (CISL) provided the computing resources (ark:/85065/d7wd3xhc). As part of the
6 CESM project, CAM-Chem is supported by the NSF and the Office of Science (BER) of the US
7 Department of Energy. This work was also sponsored by the NASA Atmospheric Composition
8 Modeling and Analysis Program Activities (ACMAP, number NNX11AH90G).

9

10 **References**

11 Allan, B. J., McFiggans, G., Plane, J. M. C., Coe, H., and McFadyen, G. G.: The nitrate radical
12 in the remote marine boundary layer, *Journal of Geophysical Research: Atmospheres*, 105,
13 24191-24204, 10.1029/2000jd900314, 2000.

14 Allan, J. D., Williams, P. I., Najera, J., Whitehead, J. D., Flynn, M. J., Taylor, J. W., Liu, D.,
15 Darbyshire, E., Carpenter, L. J., Chance, R., Andrews, S. J., Hackenberg, S. C., and McFiggans,
16 G.: Iodine observed in new particle formation events in the Arctic atmosphere during
17 ACCACIA, *Atmos. Chem. Phys.*, 15, 5599-5609, 10.5194/acp-15-5599-2015, 2015.

18 Bartis, J. T., and Widom, B.: Stochastic models of the interconversion of three or more chemical
19 species, *J. Chem. Phys.*, 60, 3474-3482, doi: 10.1063/1.1681562, 1974.

20 Butler, J. H., King, D. B., Lobert, J. M., Montzka, S. A., Yvon-Lewis, S. A., Hall, B. D.,
21 Warwick, N. J., Mondeel, D. J., Aydin, M., and Elkins, J. W.: Oceanic distributions and

1 emissions of short-lived halocarbons, *Global Biogeochem. Cycles*, 21, GB1023,
2 10.1029/2006gb002732, 2007.

3 Carpenter, L. J.: Iodine In the marine Boundary Layer, *Chem. Rev.*, 103 (12), 4953-4962, 2003.

4 Carpenter, L. J., Fleming, Z. L., Read, K. A., Lee, J. D., Moller, S. J., Hopkins, J. R., Purvis, R.
5 M., Lewis, A. C., Müller, K., Heinold, B., Herrmann, H., Fomba, K. W., Pinxteren, D., Müller,
6 C., Tegen, I., Wiedensohler, A., Müller, T., Niedermeier, N., Achterberg, E. P., Patey, M. D.,
7 Kozlova, E. A., Heimann, M., Heard, D. E., Plane, J. M. C., Mahajan, A., Oetjen, H., Ingham, T.,
8 Stone, D., Whalley, L. K., Evans, M. J., Pilling, M. J., Leigh, R. J., Monks, P. S., Karunaharan,
9 A., Vaughan, S., Arnold, S. R., Tschritter, J., Pöhler, D., Frieß, U., Holla, R., Mendes, L. M.,
10 Lopez, H., Faria, B., Manning, A. J., and Wallace, D. W. R.: Seasonal characteristics of tropical
11 marine boundary layer air measured at the Cape Verde Atmospheric Observatory, *J. Atmos.*
12 *Chem.*, 67, 87-140, 10.1007/s10874-011-9206-1, 2011.

13 Carpenter, L. J., MacDonald, S. M., Shaw, M. D., Kumar, R., Saunders, R. W., Parthipan, R.,
14 Wilson, J., and Plane, J. M. C.: Atmospheric iodine levels influenced by sea surface emissions of
15 inorganic iodine, *Nature Geosci*, 6, 108-111, 10.1038/ngeo1687, 2013.

16 Carpenter, L. J., Andrews, S. J., Lidster, R. T., Saiz-Lopez, A., Fernandez-Sanchez, M., Bloss,
17 W. J., Ouyang, B., and Jones, R. L.: A nocturnal atmospheric loss of
18 CH_2I_2 in the remote marine boundary layer, *J. Atmos. Chem.*,
19 10.1007/s10874-015-9320-6, 2015.

1 Fernandez, R. P., Salawitch, R. J., Kinnison, D. E., Lamarque, J. F., and Saiz-Lopez, A.:
2 Bromine partitioning in the tropical tropopause layer: implications for stratospheric injection,
3 *Atmos. Chem. Phys.*, 14, 13391-13410, 10.5194/acp-14-13391-2014, 2014.

4 Frisch, M., Trucks, G., Schlegel, H., Scuseria, G., Robb, M., Cheeseman, J., Scalmani, G.,
5 Barone, V., Mennucci, B., and Petersson, G.: *Gaussian 09, Revision A. 1*. Wallingford, CT:
6 Gaussian, in, Inc, 2009.

7 Georgievskii, Y., and Klippenstein, S. J.: Long-range transition state theory, *J. Chem. Phys.*, 122,
8 194103, doi: 10.1063/1.1899603, 2005.

9 Gilbert, R. G., and Smith, S. C.: *Theory of Unimolecular and Recombination Reactions*,
10 Blackwell, Oxford, 1990.

11 Glukhovtsev, M. N., Pross, A., McGrath, M. P., and Radom, L.: Extension of Gaussian-2 (G2)
12 theory to bromine- and iodine-containing molecules: Use of effective core potentials, *J. Chem.*
13 *Phys.*, 103, 1878-1885, 1995.

14 Gomez Martin, J. C., Galvez, O., Baeza-Romero, M. T., Ingham, T., Plane, J. M. C., and Blitz,
15 M. A.: On the mechanism of iodine oxide particle formation, *Phys. Chem. Chem. Phys.*, 15,
16 15612-15622, 10.1039/c3cp51217g, 2013.

17 Gómez Martín, J. C., Mahajan, A. S., Hay, T. D., Prados-Román, C., Ordóñez, C., MacDonald,
18 S. M., Plane, J. M. C., Sorribas, M., Gil, M., Paredes Mora, J. F., Agama Reyes, M. V., Oram, D.
19 E., Leedham, E., and Saiz-Lopez, A.: Iodine chemistry in the eastern Pacific marine boundary
20 layer, *Journal of Geophysical Research: Atmospheres*, 118, 887-904, 10.1002/jgrd.50132, 2013.

- 1 Großmann, K., Frieß, U., Peters, E., Wittrock, F., Lampel, J., Yilmaz, S., Tschritter, J.,
2 Sommariva, R., von Glasow, R., Quack, B., Krüger, K., Pfeilsticker, K., and Platt, U.: Iodine
3 monoxide in the Western Pacific marine boundary layer, *Atmos. Chem. Phys.*, 13, 3363-3378,
4 10.5194/acp-13-3363-2013, 2013.
- 5 Hoffmann, T., O'Dowd, C. D., and Seinfeld, J. H.: Iodine oxide homogeneous nucleation: An
6 explanation for coastal new particle production, *Geophys. Res. Lett.*, 28, 1949-1952, 2001.
- 7 Holmes, N. S., Adams, J. W., and Crowley, J. N.: Uptake and reaction of HOI and IONO₂ on
8 frozen and dry NaCl/NaBr surfaces and H₂SO₄, *Phys. Chem. Chem. Phys.*, 3, 1679-1687,
9 10.1039/b100247n, 2001.
- 10 Jones, C. E., Hornsby, K. E., Sommariva, R., Dunk, R. M., von Glasow, R., McFiggans, G., and
11 Carpenter, L. J.: Quantifying the contribution of marine organic gases to atmospheric iodine,
12 *Geophys. Res. Lett.*, 37, L18804, 2010.
- 13 Kaltsoyannis, N., and Plane, J. M. C.: Quantum chemical calculations on a selection of iodine-
14 containing species (IO, OIO, INO₃, (IO)₂, I₂O₃, I₂O₄ and I₂O₅) of importance in the atmosphere.,
15 *Phys. Chem. Chem. Phys.*, 10, 1723-1733, 2008.
- 16 Lamarque, J. F., Emmons, L. K., Hess, P. G., Kinnison, D. E., Tilmes, S., Vitt, F., Heald, C. L.,
17 Holland, E. A., Lauritzen, P. H., Neu, J., Orlando, J. J., Rasch, P. J., and Tyndall, G. K.: CAM-
18 chem: description and evaluation of interactive atmospheric chemistry in the Community Earth
19 System Model, *Geosci. Model Dev.*, 5, 369-411, 10.5194/gmd-5-369-2012, 2012.
- 20 Lawler, M. J., Mahajan, A. S., Saiz-Lopez, A., and Saltzman, E. S.: Observations of I₂ at a
21 remote marine site, *Atmos. Chem. Phys.*, 14, 2669-2678, 10.5194/acp-14-2669-2014, 2014.

1 Lee, J. D., Moller, S. J., Read, K. A., Lewis, A. C., Mendes, L., and Carpenter, L. J.: Year-round
2 measurements of nitrogen oxides and ozone in the tropical North Atlantic marine boundary layer,
3 *Journal of Geophysical Research: Atmospheres*, 114, n/a-n/a, 10.1029/2009jd011878, 2009.

4 Lee, J. D., McFiggans, G., Allan, J. D., Baker, A. R., Ball, S. M., Benton, A. K., Carpenter, L. J.,
5 Commane, R., Finley, B. D., Evans, M., Fuentes, E., Furneaux, K., Goddard, A., Good, N.,
6 Hamilton, J. F., Heard, D. E., Herrmann, H., Hollingsworth, A., Hopkins, J. R., Ingham, T.,
7 Irwin, M., Jones, C. E., Jones, R. L., Keene, W. C., Lawler, M. J., Lehmann, S., Lewis, A. C.,
8 Long, M. S., Mahajan, A., Methven, J., Moller, S. J., Müller, K., Müller, T., Niedermeier, N.,
9 O'Doherty, S., Oetjen, H., Plane, J. M. C., Pszenny, A. A. P., Read, K. A., Saiz-Lopez, A.,
10 Saltzman, E. S., Sander, R., von Glasow, R., Whalley, L., Wiedensohler, A., and Young, D.:
11 Reactive Halogens in the Marine Boundary Layer (RHAMBLE): the tropical North Atlantic
12 experiments, *Atmos. Chem. Phys.*, 10, 1031-1055, 10.5194/acp-10-1031-2010, 2010.

13 Leigh, R. J., Ball, S. M., Whitehead, J., Leblanc, C., Shillings, A. J. L., Mahajan, A. S., Oetjen,
14 H., Dorsey, J. R., Gallagher, M., Jones, R. L., Plane, J. M. C., Potin, P., and McFiggans, G.:
15 Measurements and modelling of molecular iodine emissions, transport and photodestruction in
16 the coastal region around Roscoff, *Atmos. Chem. Phys.*, 10, 11823-11838, 2010.

17 MacDonald, S. M., Gómez Martín, J. C., Chance, R., Warriner, S., Saiz-Lopez, A., Carpenter, L.
18 J., and Plane, J. M. C.: A laboratory characterisation of inorganic iodine emissions from the sea
19 surface: dependence on oceanic variables and parameterisation for global modelling, *Atmos.*
20 *Chem. Phys.*, 14, 5841-5852, 10.5194/acp-14-5841-2014, 2014.

1 Mahajan, A. S., Oetjen, H., Saiz-Lopez, A., Lee, J. D., McFiggans, G. B., and Plane, J. M. C.:
2 Reactive iodine species in a semi-polluted environment, *Geophys. Res. Lett.*, 36, L16803,
3 doi:16810.11029/12009GL038018, 2009.

4 Mahajan, A. S., Plane, J. M. C., Oetjen, H., Mendes, L., Saunders, R. W., Saiz-Lopez, A., Jones,
5 C. E., Carpenter, L. J., and McFiggans, G. B.: Measurement and modelling of tropospheric
6 reactive halogen species over the tropical Atlantic Ocean, *Atmos. Chem. Phys.*, 10, 4611-4624,
7 2010a.

8 Mahajan, A. S., Shaw, M., Oetjen, H., Hornsby, K. E., Carpenter, L. J., Kaleschke, L., Tian-
9 Kunze, X., Lee, J. D., Moller, S. J., Edwards, P., Commane, R., Ingham, T., Heard, D. E., and
10 Plane, J. M. C.: Evidence of reactive iodine chemistry in the Arctic boundary layer, *J. Geophys.*
11 *Res.*, [Atmos.], 115, D20303, doi:10.1029/2009JD013665, 2010b.

12 Mahajan, A. S., Gómez Martín, J. C., Hay, T. D., Royer, S. J., Yvon-Lewis, S., Liu, Y., Hu, L.,
13 Prados-Roman, C., Ordóñez, C., Plane, J. M. C., and Saiz-Lopez, A.: Latitudinal distribution of
14 reactive iodine in the Eastern Pacific and its link to open ocean sources, *Atmos. Chem. Phys.*, 12,
15 11609-11617, 10.5194/acp-12-11609-2012, 2012.

16 McFiggans, G., Coe, H., Burgess, R., Allan, J., Cubison, M., Alfarra, M. R., Saunders, R., Saiz-
17 Lopez, A., Plane, J. M. C., Wevill, D. J., Carpenter, L. J., Rickard, A. R., and Monks, P. S.:
18 Direct evidence for coastal iodine particles from *Laminaria* macroalgae - linkage to emissions of
19 molecular iodine, *Atmos. Chem. Phys.*, 4, 701-713, 2004.

1 Nakano, Y., Ukeguchi, H., and Ishiwata, T.: Rate constant of the reaction of NO₃ with CH₂I₂
2 measured with use of cavity ring-down spectroscopy, *Chem. Phys. Lett.*, 430, 235-239, doi:
3 10.1016/j.cplett.2006.09.002, 2006.

4 O'Dowd, C. D., Jimenez, J. L., Bahreini, R., Flagan, R. C., Seinfeld, J. H., Hameri, K., Pirjola,
5 L., Kulmala, M., Jennings, S. G., and Hoffmann, T.: Marine aerosol formation from biogenic
6 iodine emissions, *Nature*, 417, 632-636, 2002.

7 Ordóñez, C., Lamarque, J. F., Tilmes, S., Kinnison, D. E., Atlas, E. L., Blake, D. R., Sousa
8 Santos, G., Brasseur, G., and Saiz-Lopez, A.: Bromine and iodine chemistry in a global
9 chemistry-climate model: description and evaluation of very short-lived oceanic sources, *Atmos.*
10 *Chem. Phys.*, 12, 1423-1447, 10.5194/acp-12-1423-2012, 2012.

11 Plane, J. M. C., Joseph, D. M., Allan, B. J., Ashworth, S. H., and Francisco, J. S.: An
12 Experimental and Theoretical Study of the Reactions OIO + NO and OIO + OH, *J. Phys. Chem.*
13 *A*, 110, 93-100, 2006.

14 Prados-Roman, C., Cuevas, C. A., Fernandez, R. P., Kinnison, D. E., Lamarque, J. F., and Saiz-
15 Lopez, A.: A negative feedback between anthropogenic ozone pollution and enhanced ocean
16 emissions of iodine, *Atmos. Chem. Phys.*, 15, 2215-2224, 10.5194/acp-15-2215-2015, 2015a.

17 Prados-Roman, C., Cuevas, C. A., Hay, T., Fernandez, R. P., Mahajan, A. S., Royer, S. J., Galí,
18 M., Simó, R., Dachs, J., Großmann, K., Kinnison, D. E., Lamarque, J. F., and Saiz-Lopez, A.:
19 Iodine oxide in the global marine boundary layer, *Atmos. Chem. Phys.*, 15, 583-593,
20 10.5194/acp-15-583-2015, 2015b.

1 Read, K. A., Mahajan, A. S., Carpenter, L. J., Evans, M. J., Faria, B. V. E., Heard, D. E.,
2 Hopkins, J. R., Lee, J. D., Moller, S. J., Lewis, A. C., Mendes, L., McQuaid, J. B., Oetjen, H.,
3 Saiz-Lopez, A., Pilling, M. J., and Plane, J. M. C.: Extensive halogen-mediated ozone
4 destruction over the tropical Atlantic Ocean, *Nature*, 453, 1232-1235, 2008.

5 Read, K. A., Lee, J. D., Lewis, A. C., Moller, S. J., Mendes, L., and Carpenter, L. J.: Intra-annual
6 cycles of NMVOC in the tropical marine boundary layer and their use for interpreting seasonal
7 variability in CO, *Journal of Geophysical Research: Atmospheres*, 114, n/a-n/a,
8 10.1029/2009jd011879, 2009.

9 Roberston, S. H., Glowacki, D. R., Liang, C. H., Morley, C., Shannon, R., Blitz, M., and Pilling,
10 M. J.: MESMER (Master Equation Solver for Multi-Energy Well Reactions), 2008–2012: An
11 object oriented C++ program for carrying out ME calculations and eigenvalue-eigenvector
12 analysis on arbitrary multiple well systems, edited. [Available at
13 <http://sourceforge.net/projects/mesmer>.], in, 4.1 ed., 2014.

14 Roscoe, H. K., Jones, A. E., Brough, N., Weller, R., Saiz-Lopez, A., Mahajan, A. S.,
15 Schoenhardt, A., Burrows, J. P., and Fleming, Z. L.: Particles and iodine compounds in coastal
16 Antarctica, *Journal of Geophysical Research: Atmospheres*, 120, 7144-7156,
17 10.1002/2015jd023301, 2015.

18 Saiz-Lopez, A., and Plane, J. M. C.: Novel iodine chemistry in the marine boundary layer,
19 *Geophys. Res. Lett.*, 31, L04112, 2004.

20 Saiz-Lopez, A., Plane, J. M. C., Mahajan, A. S., Anderson, P. S., Bauguitte, S. J.-B., Jones, A.
21 E., Roscoe, H. K., Salmon, R. A., Bloss, W. J., Lee, J. D., and Heard, D. E.: On the vertical

1 distribution of boundary layer halogens over coastal Antarctica: implications for O₃, HO_x, NO_x
2 and the Hg lifetime, *Atmos. Chem. Phys.*, 8, 887-900, 2008.

3 Saiz-Lopez, A., Lamarque, J.-F., Kinnison, D., Tilmes, S., Ordóñez, C., Orlando, J. J., Conley,
4 A. J., Plane, J. M. C., Mahajan, A., Sousa Santos, G., Atlas, E., Blake, D. R., Sander, S. P.,
5 Schaffler, S. M., Thompson, A. M., and Brasseur, G.: Estimating the climate significance of
6 halogen-driven ozone loss in the tropical marine troposphere, *Atmos. Chem. Phys.*, 12, 3939-
7 3949, 2012a.

8 Saiz-Lopez, A., Plane, J. M. C., Baker, A. R., Carpenter, L. J., Von Glasow, R., Gómez Martín,
9 J. C., McFiggans, G., and Saunders, R. W.: Atmospheric Chemistry of Iodine, *Chem. Rev.*
10 (Washington, DC, U. S.), 112, 1773-1804, 10.1021/cr200029u, 2012b.

11 Saiz-Lopez, A., Fernandez, R. P., Ordóñez, C., Kinnison, D. E., Gómez Martín, J. C., Lamarque,
12 J. F., and Tilmes, S.: Iodine chemistry in the troposphere and its effect on ozone, *Atmos. Chem.*
13 *Phys.*, 14, 13119-13143, 10.5194/acp-14-13119-2014, 2014.

14 Saiz-Lopez, A., Baidar, S., Cuevas, C. A., Koenig, T. K., Fernandez, R. P., Dix, B., Kinnison, D.
15 E., Lamarque, J. F., Rodriguez-Lloveras, X., Campos, T. L., and Volkamer, R.: Injection of
16 iodine to the stratosphere, *Geophys. Res. Lett.*, n/a-n/a, 10.1002/2015gl064796, 2015.

17 Sander, S. P., Orkin, V. L., Kurylo, M. J., Golden, D. M., Huie, R. E., Kolb, C. E., Finlayson-
18 Pitts, B. J., Molina, M. J., Friedl, R. R., Ravishankara, A. R., Moortgat, G. K., Keller-Rudek, H.,
19 and Wine, P. H.: Chemical kinetics and photochemical data for use in atmospheric studies, JPL-
20 NASA, 2006.

1 Sherwen, T., Evans, M. J., Carpenter, L. J., Andrews, S. J., Lidster, R. T., Dix, B., Koenig, T. K.,
2 Sinreich, R., Ortega, I., Volkamer, R., Saiz-Lopez, A., Prados-Roman, C., Mahajan, A. S., and
3 Ordóñez, C.: Iodine's impact on tropospheric oxidants: a global model study in GEOS-Chem,
4 *Atmos. Chem. Phys.*, 16, 1161-1186, 10.5194/acp-16-1161-2016, 2016.

5 Simpson, W. R., Brown, S. S., Saiz-Lopez, A., Thornton, J. A., and Glasow, R. v.: Tropospheric
6 Halogen Chemistry: Sources, Cycling, and Impacts, *Chem. Rev.*, 115, 4035-4062,
7 10.1021/cr5006638, 2015.

8 Sommariva, R., Bloss, W. J., and von Glasow, R.: Uncertainties in gas-phase atmospheric iodine
9 chemistry, *Atmos. Environ.*, 57, 219-232, doi: 10.1016/j.atmosenv.2012.04.032, 2012.

10 Volkamer, R., Baidar, S., Campos, T. L., Coburn, S., DiGangi, J. P., Dix, B., Eloranta, E. W.,
11 Koenig, T. K., Morley, B., Ortega, I., Pierce, B. R., Reeves, M., Sinreich, R., Wang, S., Zondlo,
12 M. A., and Romashkin, P. A.: Aircraft measurements of BrO, IO, glyoxal, NO₂, H₂O, O₂-O₂
13 and aerosol extinction profiles in the tropics: comparison with aircraft-/ship-based in situ and
14 lidar measurements, *Atmos. Meas. Tech.*, 8, 2121-2148, 10.5194/amt-8-2121-2015, 2015.

15 von Glasow, R., Sander, R., Bott, A., and Crutzen, P. J.: Modeling halogen chemistry in the
16 marine boundary layer. 1. Cloud-free MBL, *J. Geophys. Res.*, 107, 4341, 2002.

17 Wachsmuth, M., Gäggeler, H. W., von Glasow, R., and Ammann, M.: Accommodation
18 coefficient of HOBr on deliquescent sodium bromide aerosol particles, *Atmos. Chem. Phys.*, 2,
19 121-131, 10.5194/acp-2-121-2002, 2002.

20 Wang, F., Saiz-Lopez, A., Mahajan, A. S., Gómez Martín, J. C., Armstrong, D., Lemes, M., Hay,
21 T., and Prados-Roman, C.: Enhanced production of oxidised mercury over the tropical Pacific

1 Ocean: a key missing oxidation pathway, *Atmos. Chem. Phys.*, 14, 1323-1335, 10.5194/acp-14-

2 1323-2014, 2014.

3

4

1 **Tables**

2

3 Table 1: Night time reactions of emitted inorganic iodine compounds considered in addition to
 4 the iodine chemistry scheme used by (Saiz-Lopez et al., 2014).

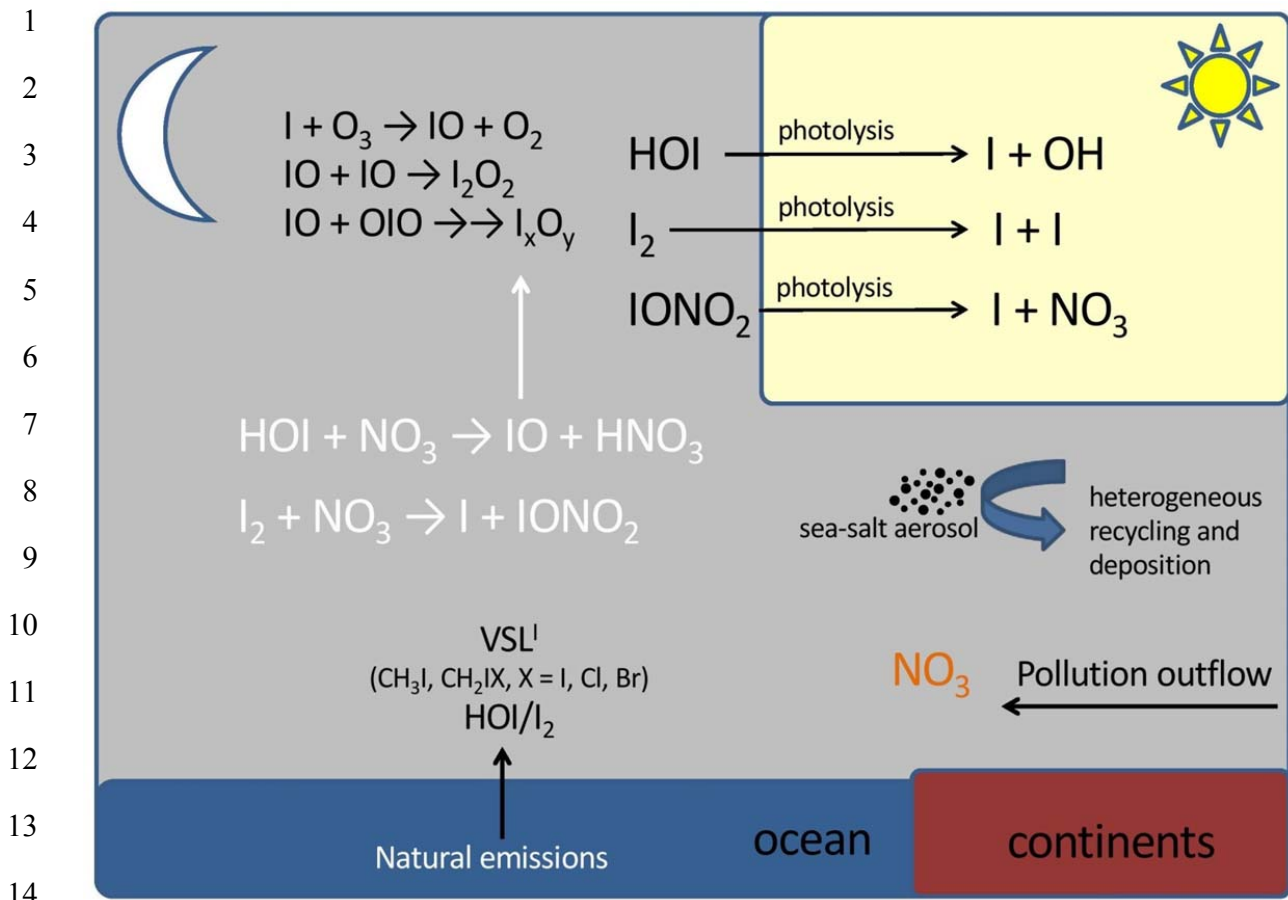
No.	Reaction	Notes
R1.	$I_2 + NO_3 \rightarrow I + IONO_2$	$1.5 \times 10^{-12} \text{ cm}^3 \text{ molecule}^{-1} \text{ s}^{-1}$ [<i>Chambers et al.</i> , 1992]
R2.	$HOI + NO_2 \rightarrow I + HNO_3$	Endothermic by 9 kJ mol^{-1} and the transition state is 73 kJ mol^{-1} above the reactants
R3.	$HOI + HNO_3 \rightarrow IONO_2 + H_2O$	Exothermic by 11 kJ mol^{-1} . The reaction first forms a complex 21 kJ mol^{-1} below the reactants but this rearranges to the products via a transition state that is 110 kJ mol^{-1} above the reactants.
R4.	$HOI + NO_3 \rightarrow IO + HNO_3$	Exothermic by 11 kJ mol^{-1} with all transition states below the reactants. $k(T) = 2.7 \times 10^{-12} (300 \text{ K} / T)^{2.66} \text{ cm}^3 \text{ molecule}^{-1} \text{ s}^{-1}$

5
6

1 **Table 2.** Calculated vibrational frequencies, rotational constants and energies of the stationary
 2 points and asymptotes on the HOI + NO₃ doublet potential energy surface

Species	Geometry ^a	Vibrational frequencies ^b	Rotational constants ^c	Potential energy ^d
HOI + NO ₃		603, 1084, 3803 & 261, 261, 805, 1108, 1108, 1126	623.9, 8.182, 8.076 & 13.84, 13.84, 6.919	0.0
IOH-NO ₃ complex	O 1.623, 0.284, -0.331 H 1.484, -0.657, -0.043 I 0.009, 1.205, 0.286 N -0.456, -2.265, 0.030 O -1.052, -3.321, -0.0473 O -1.147, -1.195, -0.228 O 0.742, -2.161, 0.333	55, 84, 118, 161, 196, 615, 629, 667, 705, 803, 968, 1228, 1273, 1491, 3268	5.610, 0.916, 0.806	-24.0
IO-H-NO ₂ TS	O 0.309, 1.515, 0.247 H -0.834, 1.314, -0.017 I 1.280, -0.089, -0.093 N -2.349, -0.133, 0.019 O -3.518, -0.429, -0.035 O -1.444, -0.962, 0.257 O -2.019, 1.117, -0.187	1249i, 70, 97, 103, 225, 472, 676, 698, 797, 806, 1041, 1147, 1308, 1513, 1626	6.300, 0.864, 0.767	-16.4
IO-HNO ₃ complex	O 0.571, 1.350, 0.348 H -1.111, 1.098, -0.020 I 1.870, 0.0645, -0.152 N -2.503, -0.202, 0.0186 O -3.673, -0.396, -0.170 O -1.654, -0.986, 0.401 O -2.081, 1.090, -0.242	35, 43, 76, 126, 198, 623, 677, 703, 772, 798, 939, 1331, 1416, 1713, 3281	7.058, 0.605, 0.566	-34.8
IO + HNO ₃		648 & 477, 585, 649, 782, 901, 1320, 1345, 1738, 3724	9.844 & 13.01, 12.05, 6.258	-10.6

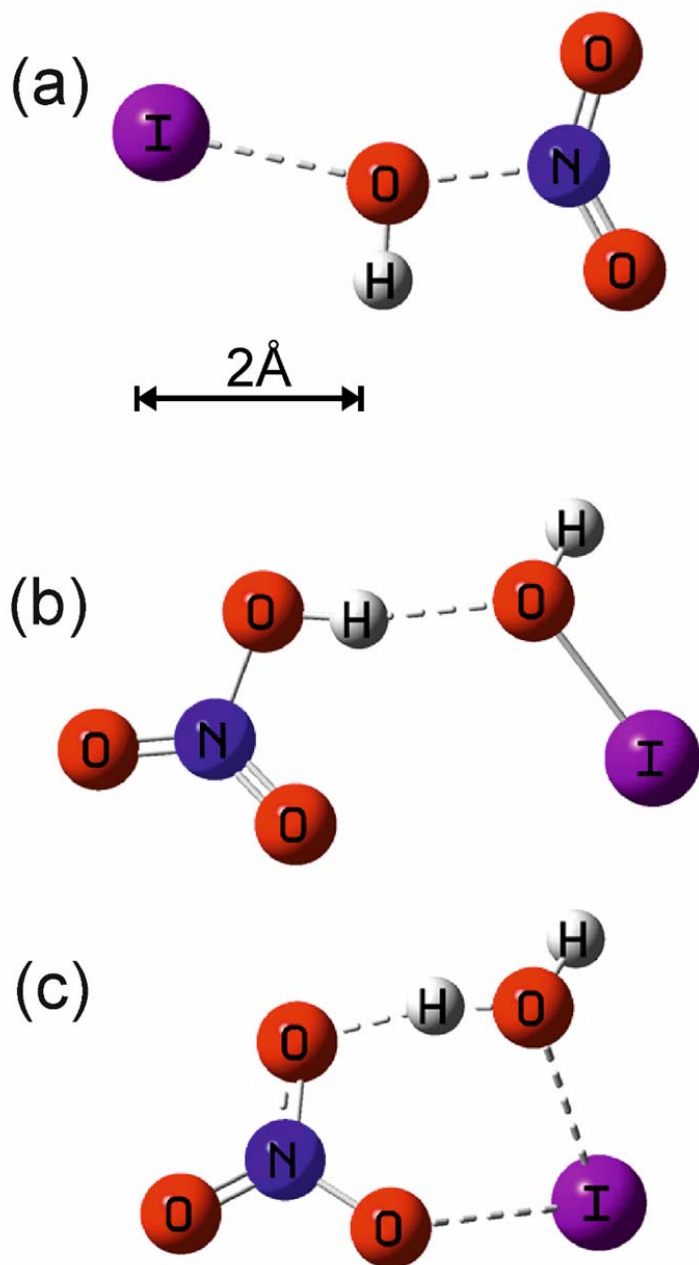
3 ^a Cartesian co-ordinates in Å. ^b In cm⁻¹. ^c In GHz. ^d In kJ mol⁻¹, including zero-point energy and spin-
 4 orbit coupling of I and IO (see text).



15 **Figure 1.** New nocturnal iodine chemistry (in white) implemented in the THAMO and CAM-
16 Chem models.

17
18
19
20
21
22
23
24
25

1



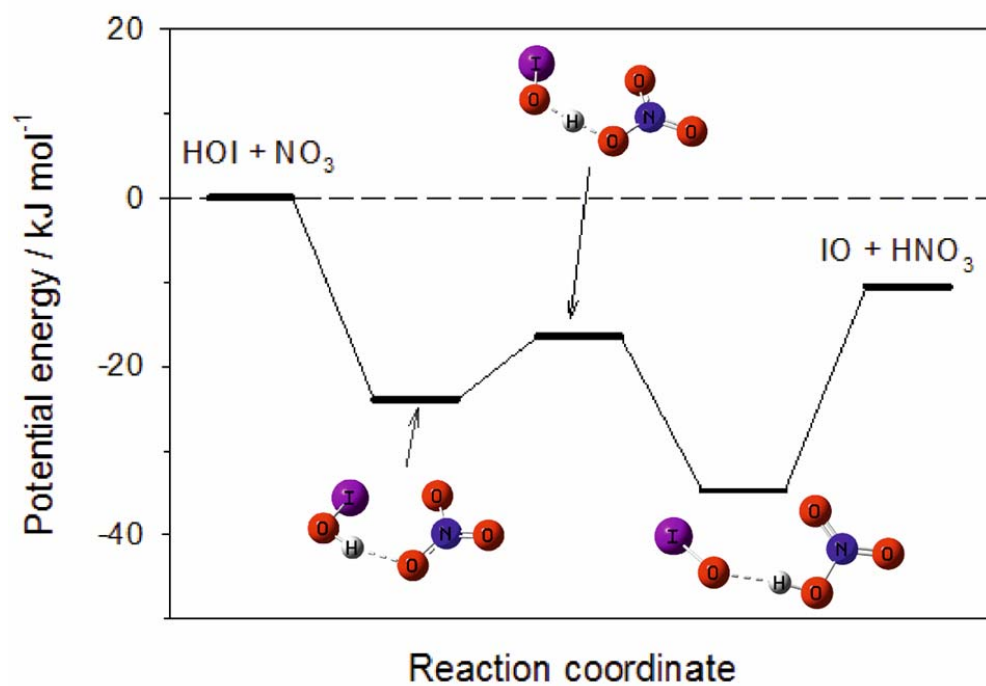
2

3

4

5 **Figure 2:** (a) Transition state for the reaction between HOI and NO₂ to form HNO₃ + I; (b)
6 complex formed between HOI and HNO₃, which then reacts via transition state (c) to form
7 IONO₂ + H₂O.

1

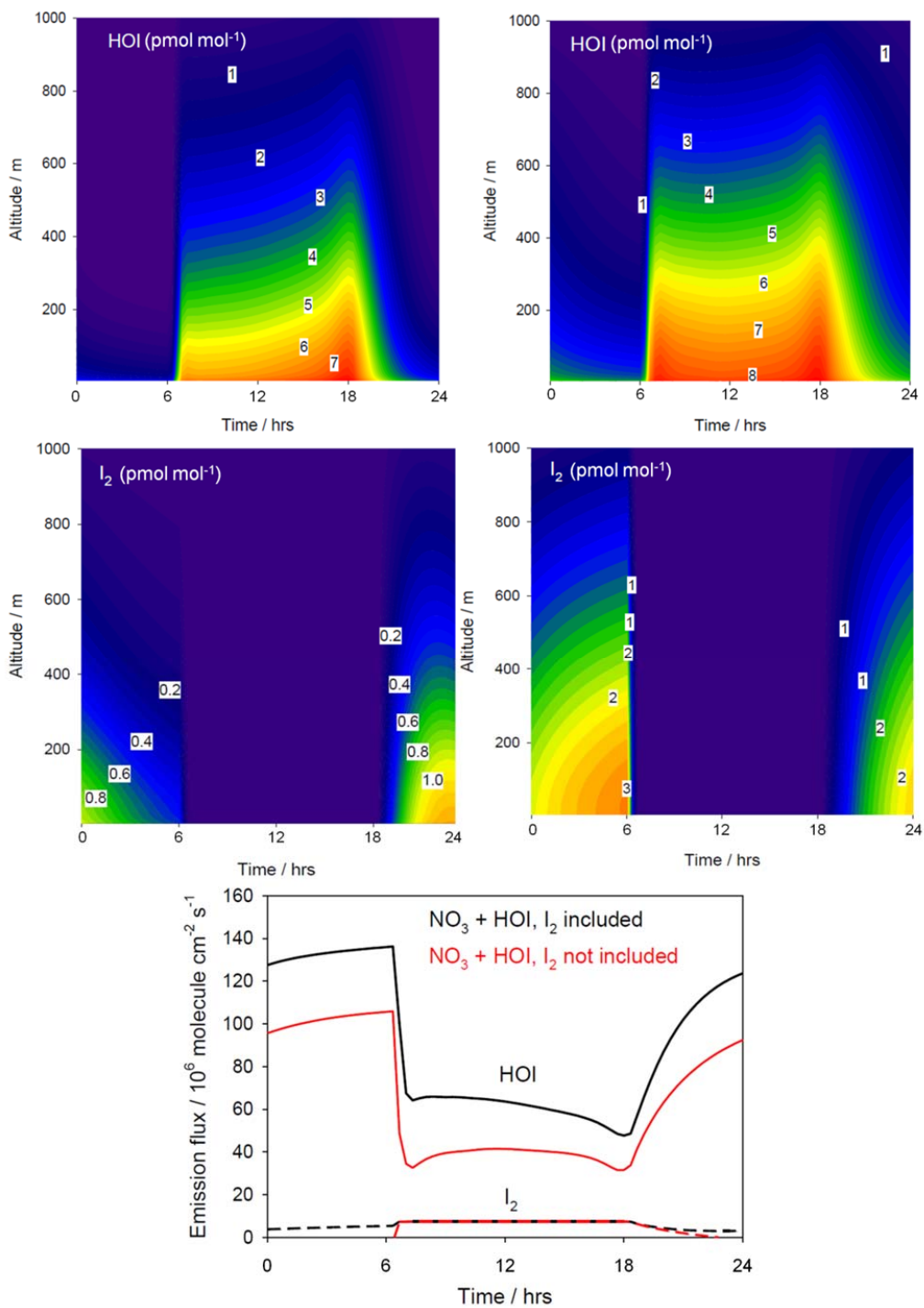


2

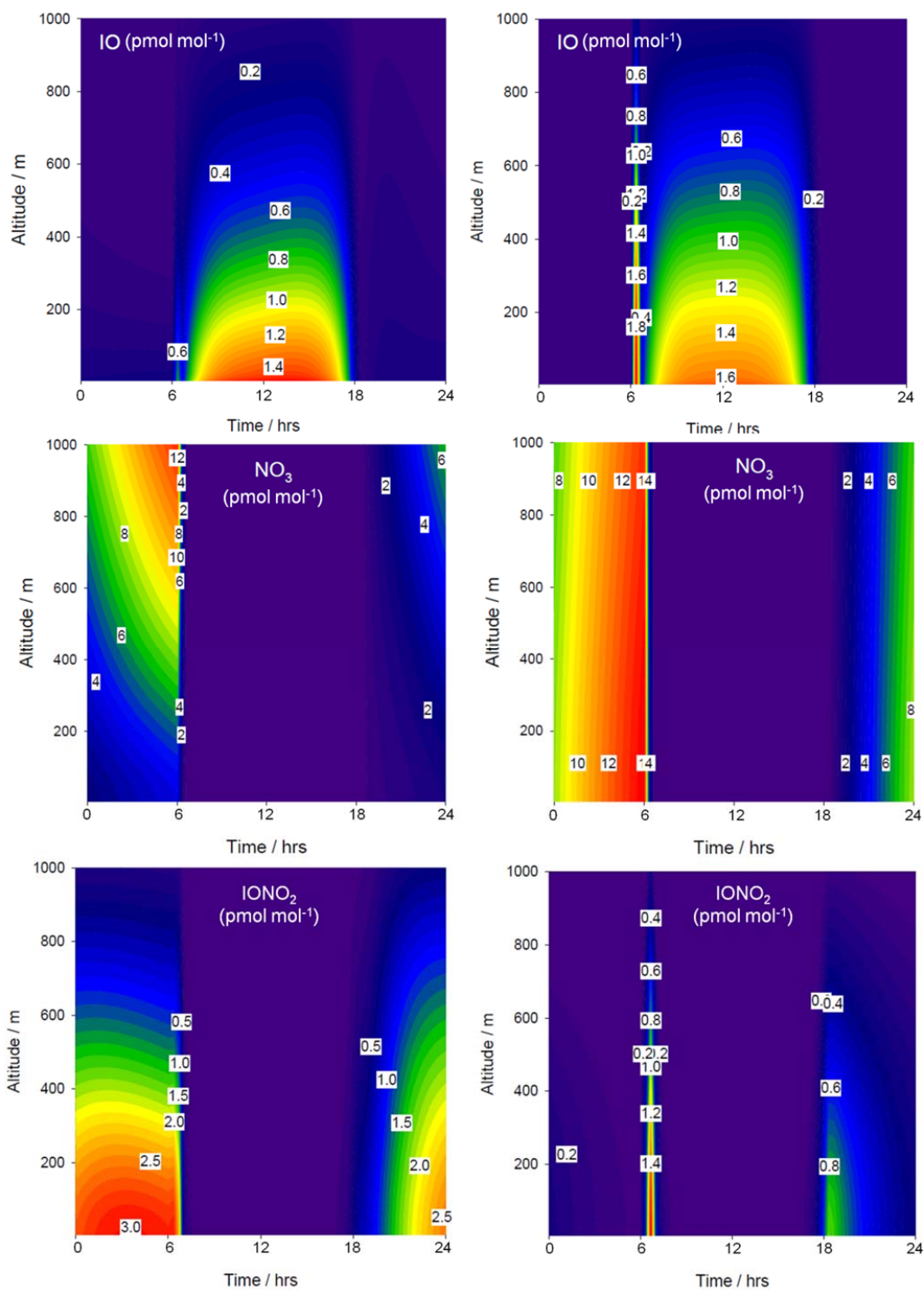
3

4 **Figure 3.** Potential energy surface for the reaction between HOI and NO₃, which contains two
5 intermediate complexes separated by a submerged barrier.

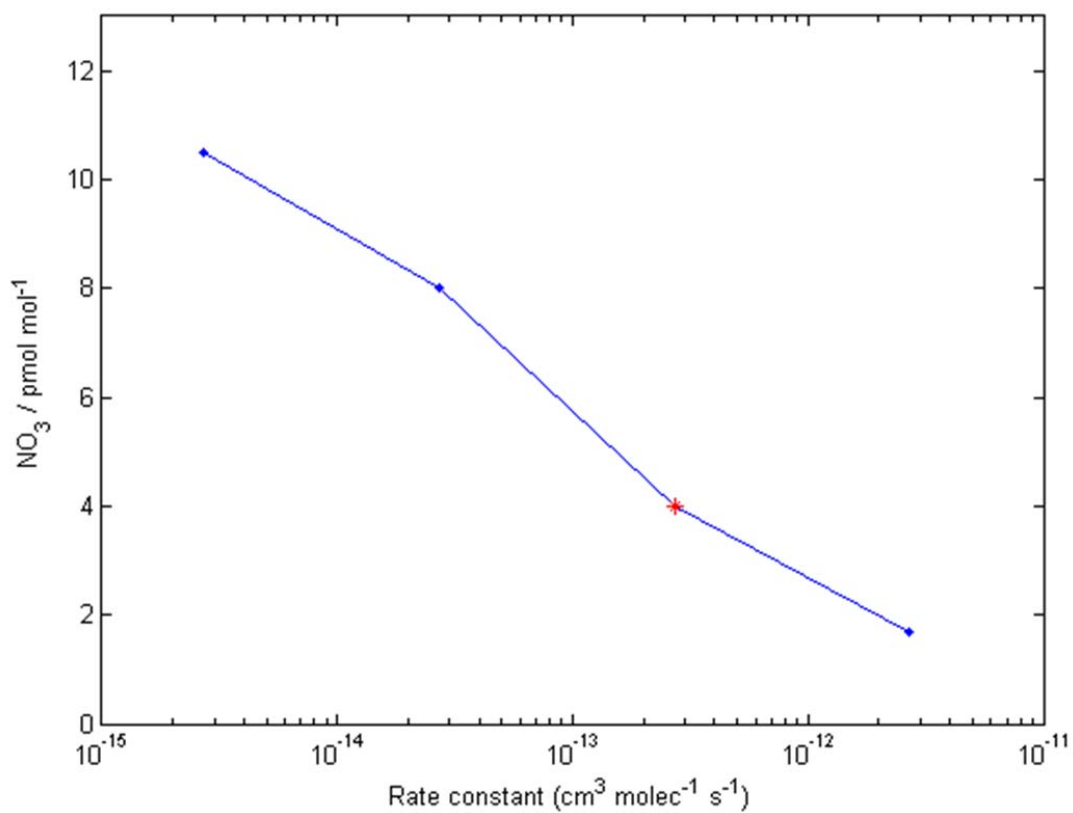
6



1
 2 **Figure 4.** THAMO modeled diurnal variation of HOI, I₂ (upper panels) and the HOI/I₂ flux from
 3 the ocean surface (bottom panel). The right hand panels are from scenario 1, which do not
 4 include night time reactions of HOI and I₂ with NO₃, while the left hand panels include the
 5 reactions in scenario 2. In bottom panel red lines represent scenario 1, while black lines
 6 correspond to scenario 2.

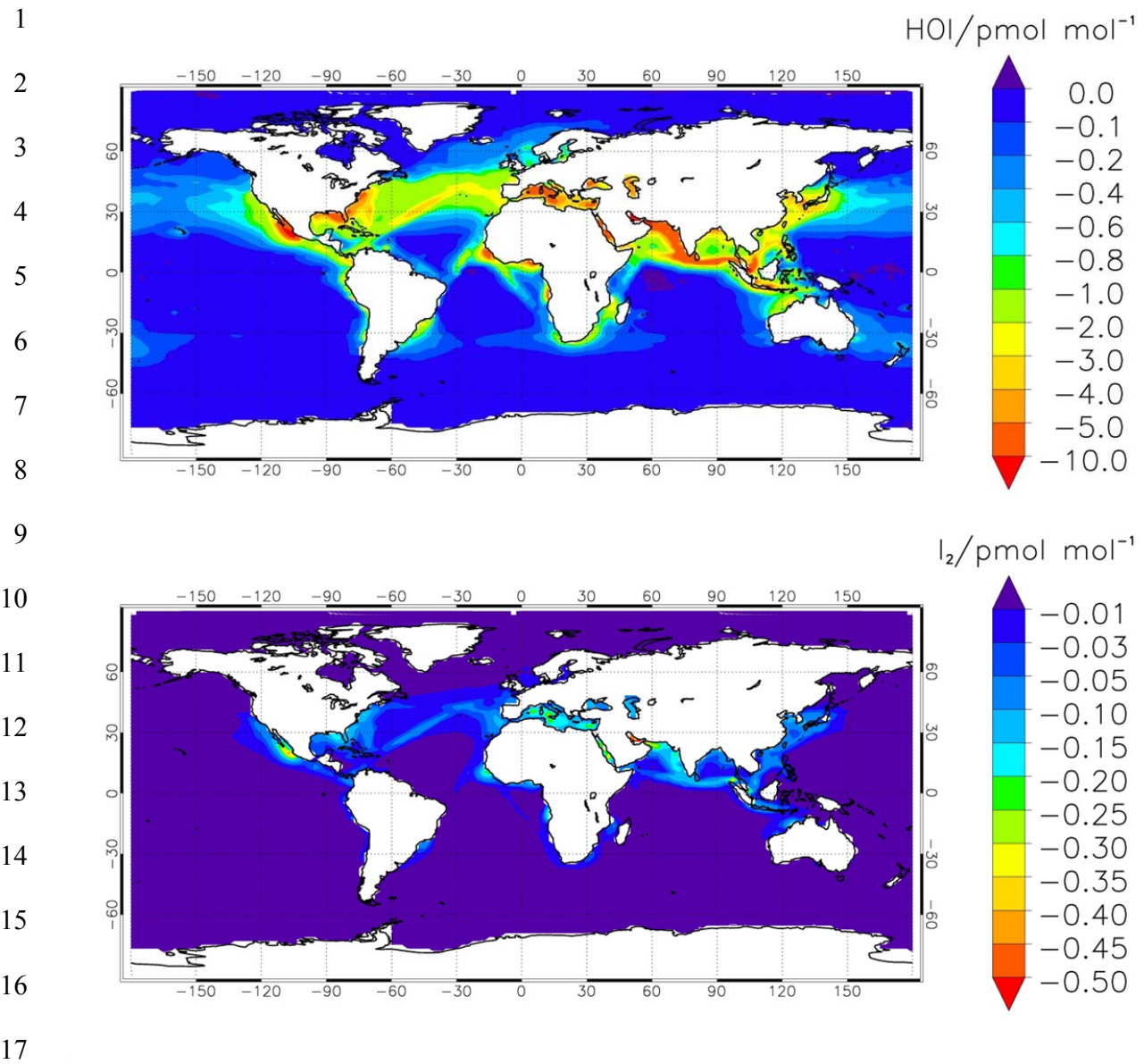


1
 2 **Figure 5.** THAMO modeled diurnal variation of IO, NO₃ and the IONO₂. The right hand panels
 3 are from scenario 1, which do not include night time reactions of HOI and I₂ with NO₃, while the
 4 left hand panels include the reactions in scenario 2.



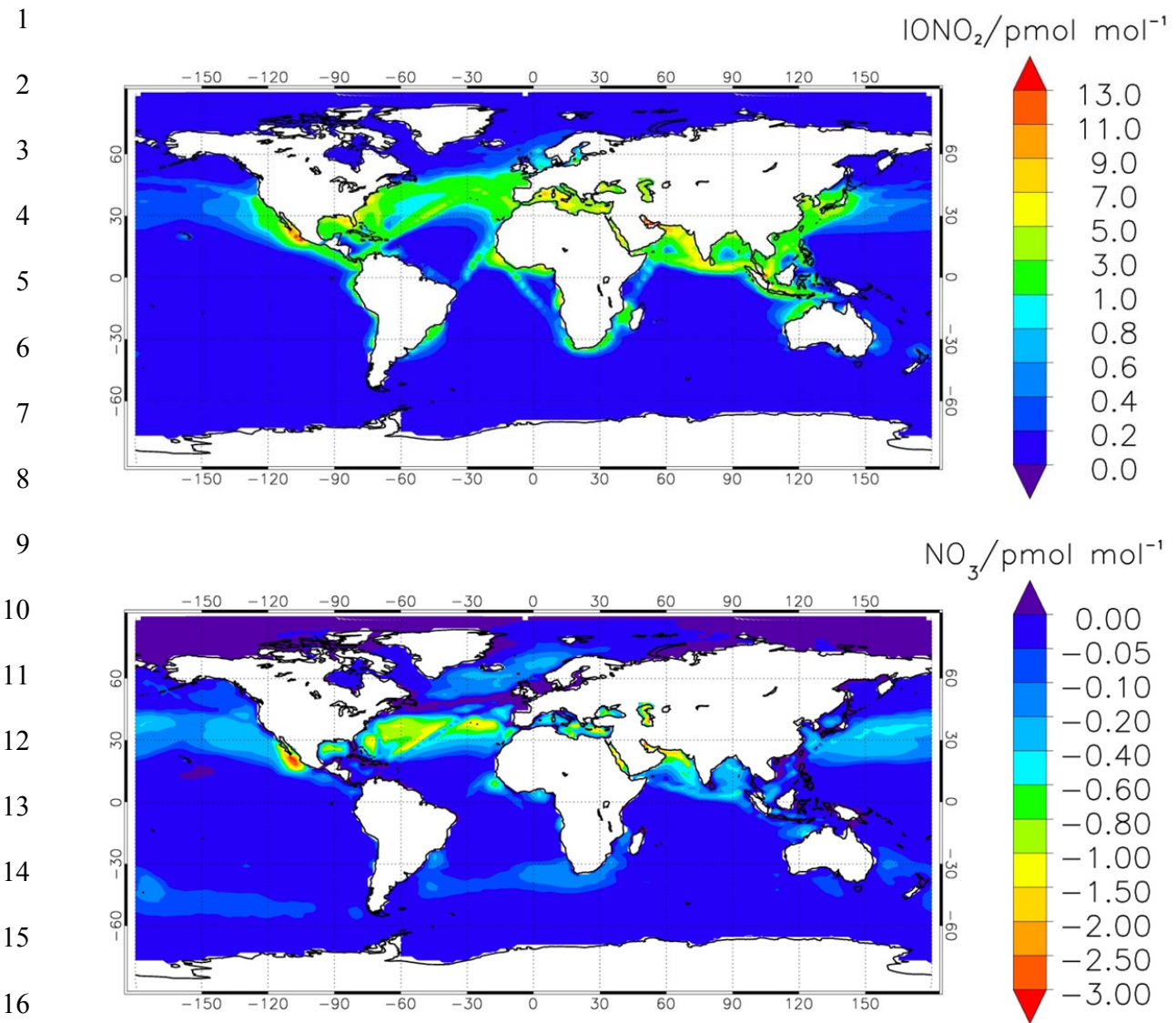
1
2 **Figure 6.** Sensitivity run showing the effect of the uncertainty in the rate constant estimation on
3 the reduction of NO₃ at the surface - the red point is the theoretical estimate.

4
5
6
7
8
9
10
11



18 **Figure 7.** Modelled annual average of HOI (a) and I_2 (b) during night time at the surface level.
 19 The panels show the difference in volume mixing ratio between the simulations with and without
 20 reactions (1) and (4).

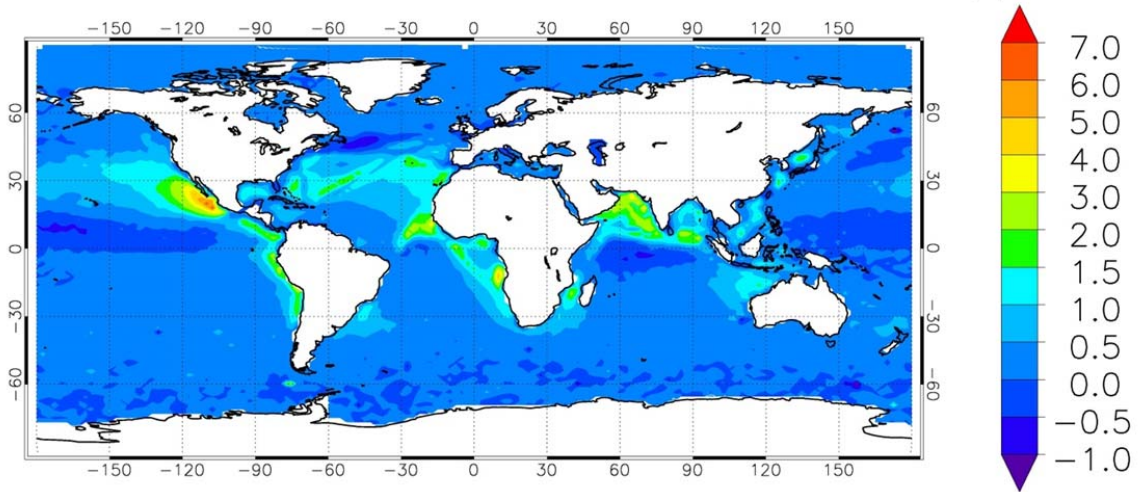
21



18 **Figure 8.** Modelled annual average of IONO_2 (a) and NO_3 (b) during night time [at the surface](#)
 19 [level](#), as the difference in volume mixing ratio between the simulations with and without
 20 reactions (1) and (4).

21

DMS/ $\mu\text{mol mol}^{-1}$



1
2
3
4
5
6
7
8
9
10
11
12
13
14
15
16
17
18
19
20
21
22
23
24

Figure 9. Increase in the DMS levels during night time at the surface level due to the inclusion of the reactions R1 and R4 in CAM-Chem.

1
2
3
4
5
6
7
8
9
10
11
12
13
14
15
16
17
18
19
20
21
22
23
24

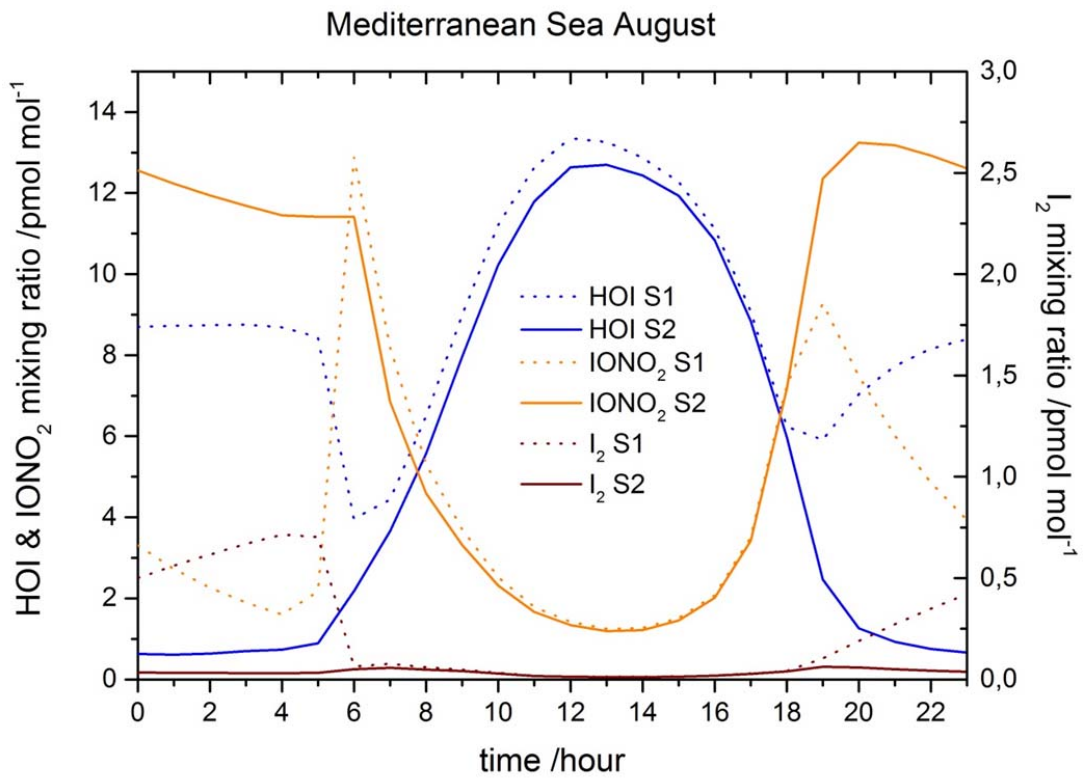
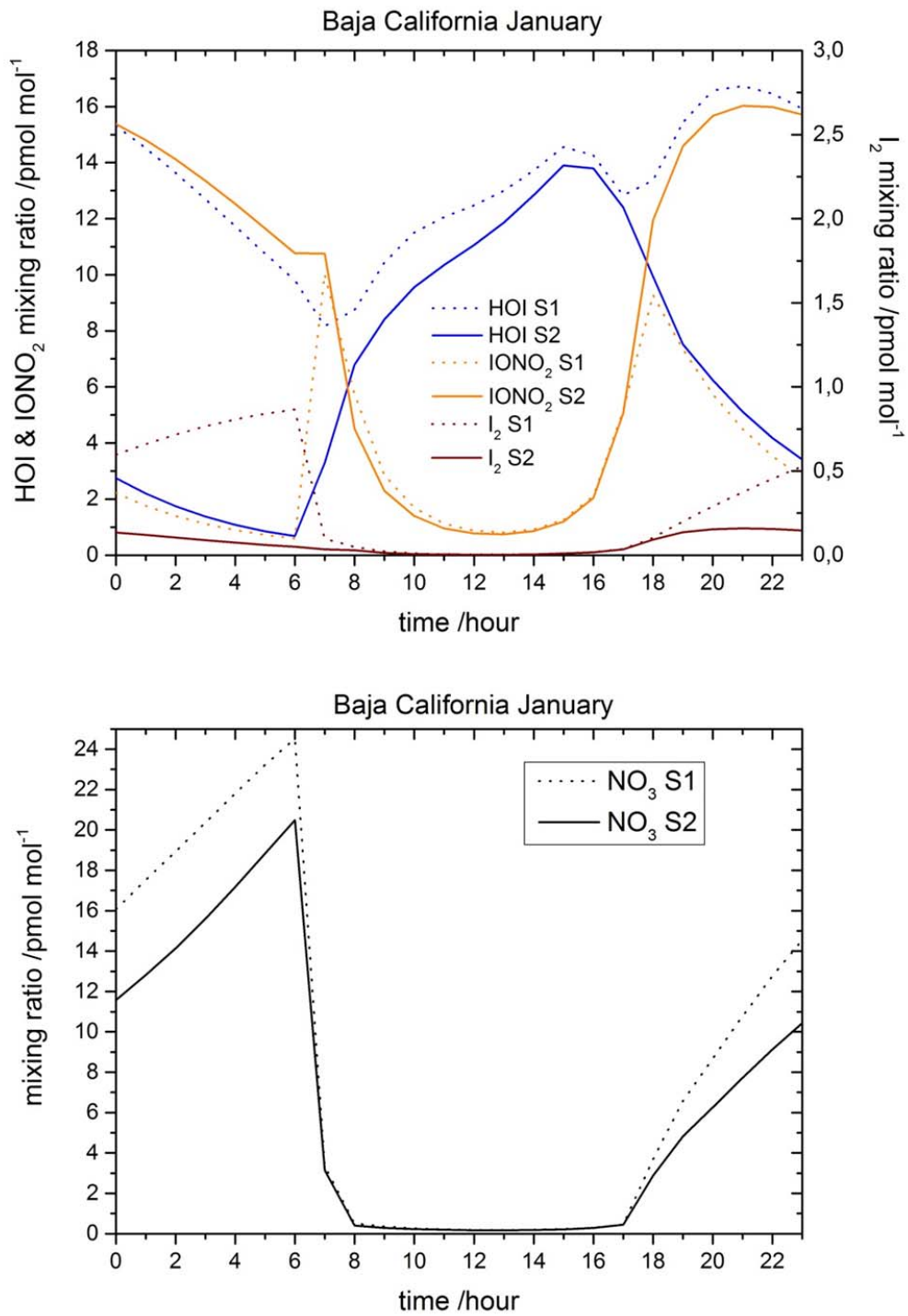


Figure 10. Hourly averaged concentration of HOI, IONO₂ and I₂ in the Mediterranean Sea at the surface level (lon:10°→20°E, lat:33°→40°N)

1
2
3
4
5
6
7
8
9
10
11
12
13
14
15
16
17
18
19
20
21



22 **Figure 11.** Hourly averaged concentration of HOI, IONO₂ and I₂ (upper panel) and NO₃ (bottom
23 panel) in the Pacific Ocean at the south of Baja California peninsula at the surface level
24 (lon: -110°→-106°E, lat:16°→23°N)

Supplementary information for

Iodine chemistry after dark

Alfonso Saiz-Lopez¹, John M.C. Plane², Carlos A. Cuevas¹, Anoop S. Mahajan³,
Jean-François Lamarque⁴ and Douglas E. Kinnison⁴

¹Department of Atmospheric Chemistry and Climate, Institute of Physical Chemistry Rocasolano, CSIC, Madrid, Spain

²School of Chemistry, University of Leeds, Leeds, UK

³Indian Institute of Tropical Meteorology, Pune, India

⁴Atmospheric Chemistry Observations and Modelling, NCAR, Colorado, USA

Correspondence to: A. Saiz-Lopez (a.saiz@csic.es)

Table 1. Iodine chemistry scheme in CAM-Chem: Bimolecular, thermal decomposition and termolecular reactions.

Reaction	$k / \text{cm}^3 \text{ molecule}^{-1} \text{ s}^{-1}$	Notes
$\text{I} + \text{O}_3 \rightarrow \text{IO} + \text{O}_2$	$2.1 \times 10^{-11} e^{(-830/T)}$	1
$\text{IO} + \text{O}_3 \rightarrow \text{OIO} + \text{O}_2$	3.6×10^{-16}	2
$\text{I} + \text{HO}_2 \rightarrow \text{HI} + \text{O}_2$	$1.5 \times 10^{-11} e^{(-1090/T)}$	3
$\text{IO} + \text{NO} \rightarrow \text{I} + \text{NO}_2$	$7.15 \times 10^{-12} e^{(300/T)}$	1
$\text{IO} + \text{HO}_2 \rightarrow \text{HOI} + \text{O}_2$	$1.4 \times 10^{-11} e^{(540/T)}$	1
$\text{IO} + \text{IO} \rightarrow \text{OIO} + \text{I}$	$2.13 \times 10^{-11} e^{(180/T)} \times [1 + e^{(-p/191.42)}]$	1, 4
$\text{IO} + \text{IO} \rightarrow \text{I}_2\text{O}_2$	$3.27 \times 10^{-11} e^{(180/T)} \times [1 - 0.65 e^{(-p/191.42)}]$	1, 4
$\text{IO} + \text{OIO} \rightarrow \text{I}_2\text{O}_3$	$w_1 \cdot \exp(w_2 \cdot T)^a$	4, 5, 6 ^g
$\text{OIO} + \text{OIO} \rightarrow \text{I}_2\text{O}_4$	$w_1 \cdot \exp(w_2 \cdot T)^b$	4, 5, 6 ^g
$\text{I}_2 + \text{O} \rightarrow \text{IO} + \text{I}$	1.25×10^{-10}	1
$\text{IO} + \text{O} \rightarrow \text{I} + \text{O}_2$	1.4×10^{-10}	1
$\text{IO} + \text{OH} \rightarrow \text{HO}_2 + \text{I}$	1.0×10^{-10}	7
$\text{I}_2\text{O}_2 \rightarrow \text{OIO} + \text{I}$	$w_1 \cdot \exp(w_2/T)^c$	5, 6, 8 ^g
$\text{I}_2\text{O}_2 \rightarrow \text{IO} + \text{IO}$	$w_1 \cdot \exp(w_2/T)^d$	5, 6, 8 ^g
$\text{I}_2\text{O}_4 \rightarrow 2 \text{OIO}$	$w_1 \cdot \exp(w_2/T)^e$	5, 8 ^g
$\text{I}_2 + \text{OH} \rightarrow \text{HOI} + \text{I}$	1.8×10^{-10}	3
$\text{I}_2 + \text{NO}_3 \rightarrow \text{I} + \text{IONO}_2$	1.5×10^{-12}	9
$\text{I} + \text{NO}_3 \rightarrow \text{IO} + \text{NO}_2$	1.0×10^{-10}	1
$\text{OH} + \text{HI} \rightarrow \text{I} + \text{H}_2\text{O}$	$1.6 \times 10^{-11} e^{(440/T)}$	1
$\text{I} + \text{IONO}_2 \rightarrow \text{I}_2 + \text{NO}_3$	$9.1 \times 10^{-11} e^{(-146/T)}$	5
$\text{HOI} + \text{OH} \rightarrow \text{IO} + \text{H}_2\text{O}$	2.0×10^{-13}	10
$\text{IO} + \text{DMS} \rightarrow \text{DMSO} + \text{I}$	$3.2 \times 10^{-13} e^{(-925/T)}$	11
$\text{INO}_2 \rightarrow \text{I} + \text{NO}_2$	$1008 \times 10^{15} e^{(-13670/T)}$	12, 13, 14
$\text{IONO}_2 \rightarrow \text{IO} + \text{NO}_2$	$w_1 \cdot \exp(w_2/T)^f$	5, 15
$\text{INO} + \text{INO} \rightarrow \text{I}_2 + 2\text{NO}$	$8.4 \times 10^{-11} e^{(-2620/T)}$	3
$\text{INO}_2 + \text{INO}_2 \rightarrow \text{I}_2 + 2\text{NO}_2$	$4.7 \times 10^{-13} e^{(-1670/T)}$	1
$\text{OIO} + \text{NO} \rightarrow \text{IO} + \text{NO}_2$	$1.1 \times 10^{-12} e^{(542/T)}$	14
$\text{HI} + \text{NO}_3 \rightarrow \text{I} + \text{HNO}_3$	$1.3 \times 10^{-12} e^{(-1830/T)}$	16
$\text{IO} + \text{BrO} \rightarrow \text{Br} + \text{I} + \text{O}_2$	$0.30 \times 10^{-11} e^{(510/T)}$	1
$\text{IO} + \text{BrO} \rightarrow \text{Br} + \text{OIO}$	$1.20 \times 10^{-11} e^{(510/T)}$	1
$\text{I} + \text{BrO} \rightarrow \text{IO} + \text{Br}$	1.44×10^{-11}	17, 18, 19

$\text{IO} + \text{ClO} \rightarrow \text{I} + \text{OCIO}$	$2.585 \times 10^{-12} e^{(280/T)}$	1
$\text{IO} + \text{ClO} \rightarrow \text{I} + \text{Cl} + \text{O}_2$	$1.175 \times 10^{-12} e^{(280/T)}$	1
$\text{IO} + \text{ClO} \rightarrow \text{ICl} + \text{O}_2$	$0.940 \times 10^{-12} e^{(280/T)}$	1
$\text{IO} + \text{Br} \rightarrow \text{I} + \text{BrO}$	2.49×10^{-11}	18, 19
$\text{IO} + \text{NO}_3 \rightarrow \text{OIO} + \text{NO}_2$	9.0×10^{-12}	20
$\text{IO} + \text{CH}_3\text{O}_2 \rightarrow \text{CH}_2\text{O} + \text{I} + \text{HO}_2$	2.0×10^{-12}	2 ^h
$\text{CH}_3\text{I} + \text{OH} \rightarrow \text{I} + \text{H}_2\text{O} + \text{HO}_2$	$2.90 \times 10^{-12} e^{(-1100/T)}$	3
$\text{I} + \text{NO}_2 (+ \text{M}) \rightarrow \text{INO}_2 (+ \text{M})$	$k_0 = 3 \times 10^{-31} \times (\text{T} / 300)^{-1}$ $k_\infty = 6.6 \times 10^{-11}$	3 ⁱ
$\text{IO} + \text{NO}_2 (+ \text{M}) \rightarrow \text{IONO}_2 (+ \text{M})$	$k_0 = 6.5 \times 10^{-31} \times (\text{T} / 300)^{-3.5}$ $k_\infty = 7.6 \times 10^{-12} \times (\text{T} / 300)^{-1.5}$	3 ⁱ
$\text{I} + \text{NO} (+ \text{M}) \rightarrow \text{INO} (+ \text{M})$	$k_0 = 1.8 \times 10^{-32} \times (\text{T} / 300)^{-1}$ $k_\infty = 1.7 \times 10^{-11}$	3 ⁱ
$\text{OIO} + \text{OH} (+ \text{M}) \rightarrow \text{HOIO}_2 (+ \text{M})$	$k_0 = 1.5 \times 10^{-27} \times (\text{T} / 300)^{-3.93}$ $k_\infty = 7.76 \times 10^{-10} \times (\text{T} / 300)^{-0.8}$	14 ^j
$\text{HOI} + \text{NO}_3 \rightarrow \text{IO} + \text{HNO}_3$	$2.7 \times 10^{-12} (300/\text{T})^{2.66}$	21

¹ IUPAC-2008 (Atkinson et al., 2007) ; ²(Dillon et al., 2006b); ³ JPL-2010 (Sander et al., 2011); ⁴(Gómez Martín et al., 2007); ⁵(Kaltsoyannis and Plane, 2008); ⁶(Galvez et al., 2013); ⁷(Bösch et al., 2003); ⁸ (Gómez Martín and Plane, 2009); ⁹(Chambers et al., 1992); ¹⁰(Chameides and Davis, 1980); ¹¹(Dillon et al., 2006a); ¹²(McFiggans et al., 2000); ¹³(Jenkin et al., 1985); ¹⁴(Plane et al., 2006); ¹⁵(Allan and Plane, 2002); ¹⁶(Lancar et al., 1991); ¹⁷(Laszlo et al., 1997); ¹⁸(Bedjanian et al., 1997); ¹⁹(Gilles et al., 1997); ²⁰(Dillon et al., 2008); ²¹This work.

$$^a \quad w1 = 4.687 \times 10^{-10} - 1.3855 \times 10^{-5} \times e^{(-0.75 \text{ p} / 1.62265)} + 5.51868 \times 10^{-10} \times e^{(-0.75 \text{ p} / 199.328)}$$

$$w2 = -0.00331 - 0.00514 \times e^{(-0.75 \text{ p} / 325.68711)} - 0.00444 \times e^{(-0.75 \text{ p} / 40.81609)}$$

$$^b \quad w1 = 1.1659 \times 10^{-9} - 7.79644 \times 10^{-10} \times e^{(-0.75 \text{ p} / 22.09281)} + 1.03779 \times 10^{-9} \times e^{(-0.75 \text{ p} / 568.15381)}$$

$$w2 = -0.00813 - 0.00382 \times e^{(-0.75 \text{ p} / 45.57591)} - 0.00643 \times e^{(-0.75 \text{ p} / 417.95061)}$$

$$^c \quad w1 = 3.54288 \times 10^{10} + 1.8523 \times 10^{11} \times 0.75 \text{ p} - 1.45435 \times 10^8 \times (0.75 \text{ p})^2 + 60799.4344 \times (0.75 \text{ p})^3$$

$$w2 = -9681.65989 + 346.95538 \times e^{(-0.75 \text{ p} / 343.25322)} + 251.78032 \times e^{(-0.75 \text{ p} / 44.1466)}$$

$$^d \quad w1 = 255335000000 - 4418880000 \times 0.75 \text{ p} + 85618600 \times (0.75 \text{ p})^2 + 14218.81 \times (0.75 \text{ p})^3$$

$$w2 = -11466.82304 + 597.01334 \times e^{(-0.75 \text{ p} / 1382.62325)} - 167.3391 \times e^{(-0.75 \text{ p} / 43.75089)}$$

$$^e \quad w1 = -1.92626 \times 10^{14} + 4.67414 \times 10^{13} \times 0.75 \text{ p} - 3.68651 \times 10^8 \times (0.75 \text{ p})^2 - 3.09109 \times 10^6 \times (0.75 \text{ p})^3$$

$$w2 = -12302.15294 + 252.78367 \times e^{(-0.75 \text{ p} / 46.12733)} + 437.62868 \times e^{(-0.75 \text{ p} / 428.4413)}$$

$$\begin{aligned}
 {}^f \quad w_1 &= -2.63544 \times 10^{13} + 4.32845 \times 10^{12} \times (0.75 \text{ p}) + 3.73758 \times 10^8 \times (0.75 \text{ p})^2 - \\
 &628468.76313 \times (0.75 \text{ p})^3 \\
 w_2 &= -13847.85015 + 240.34465 \times e^{(-0.75 \text{ p} / 49.27141)} + 451.35864 \times e^{(-0.75 \text{ p} / \\
 &436.87605)}
 \end{aligned}$$

^g The empirical expressions of the form $w_1 \cdot \exp(w_2 \cdot T)$ were obtained by non-linear least squares fitting of *Rice–Ramsperger–Kassel–Marcus* (RRKM) theoretical results for the indicated reaction rate constants and thermal dissociation rates in the (27 – 1013) hPa pressure range. RRKM calculations were carried out using the MESMER algorithm (Glowacki et al., 2012) as indicated in the corresponding references (e.g. (Galvez et al., 2013)). Expression ^a produces negative values outside the range of modelled rate constants ($p < 20$ hPa), and therefore a fixed rate constant of $3 \times 10^{-11} \text{ cm}^3 \text{ molecule}^{-1} \text{ s}^{-1}$ was assumed. Expressions ^e and ^f generate negligible dissociation rates below ~ 500 hPa which become negative at ~ 8 hPa – in this case they are set to zero below that pressure.

^h Updated heats of formation for IO, OIO, and CH_3O_2 (Dooley et al., 2008; Gómez Martín and Plane, 2009; Knyazev and Slagle, 1998) show that the only accessible exothermic product channel of $\text{CH}_3\text{O}_2 + \text{IO}$ (Drougas and Kosmas, 2007) is $\text{CH}_2\text{O} + \text{I} + \text{O}_2$ ($\Delta H_r = -5 \pm 6 \text{ kJ mol}^{-1}$), consistent with the high yield of I and low yield of OIO found experimentally (Bale et al., 2005; Enami et al., 2006). Sensitivity studies have been carried out (Saiz-Lopez et al., 2014) using the preferred rate constant for this reaction of $2 \times 10^{-12} \text{ cm}^3 \text{ molecule}^{-1} \text{ s}^{-1}$ (Dillon et al., 2006b), resulting in an enhancement of the ozone loss of 0.5% in the MBL and of less than 0.1% integrated throughout the troposphere in the J_{IxO_y} scenario, and similarly negligible enhancements in the Base scenario. Impacts in the I_y partitioning are also very minor.

ⁱ The temperature and pressure dependent rate constant (k) is computed based on the low pressure (k_0) and the high-pressure (k_∞) rate coefficients following JPL-2010 (Sander et al., 2011).

^j The Fast rate constants and a thermally stable product HOIO_2 have been predicted theoretically (Plane et al., 2006), but no experimental studies reporting observation of HOIO_2 and its photochemical properties in the gas phase are available. Since the level of uncertainty is even larger than for the I_xO_y , it has not been included in the mechanism.

Table 2. Iodine chemistry scheme in CAM-Chem: Photochemical reactions.

Reaction
$\text{CH}_3\text{I} + h\nu \rightarrow \text{CH}_3\text{O}_2 + \text{I}$
$\text{CH}_2\text{I}_2 + h\nu \rightarrow 2\text{I}^a$
$\text{CH}_2\text{IBr} + h\nu \rightarrow \text{Br} + \text{I}^a$
$\text{CH}_2\text{ICl} + h\nu \rightarrow \text{Cl} + \text{I}^a$
$\text{I}_2 + h\nu \rightarrow 2\text{I}$
$\text{IO} + h\nu \rightarrow \text{I} + \text{O}$
$\text{OIO} + h\nu \rightarrow \text{I} + \text{O}_2$
$\text{INO} + h\nu \rightarrow \text{I} + \text{NO}$
$\text{INO}_2 + h\nu \rightarrow \text{I} + \text{NO}_2^b$
$\text{IONO}_2 + h\nu \rightarrow \text{I} + \text{NO}_3$
$\text{HOI} + h\nu \rightarrow \text{I} + \text{OH}$
$\text{IBr} + h\nu \rightarrow \text{I} + \text{Br}$
$\text{ICl} + h\nu \rightarrow \text{I} + \text{Cl}$
$\text{I}_2\text{O}_2 + h\nu \rightarrow \text{I} + \text{OIO}^c$
$\text{I}_2\text{O}_3 + h\nu \rightarrow \text{IO} + \text{OIO}^c$
$\text{I}_2\text{O}_4 + h\nu \rightarrow \text{OIO} + \text{OIO}^c$

Photolysis rates are computed online considering the actinic flux calculation in CAM-Chem. The absorption cross-sections and quantum yields for all species besides the I_xO_y have been taken from IUPAC-2008 (Atkinson et al., 2007; Atkinson et al., 2008) and JPL-2010 (Sander et al., 2011).

^a radical organic products are not considered.

^b only the reaction channel reported in JPL 06-02 (Sander et al., 2006) is considered.

^c photolysis reactions only considered in the $J_{\text{I}x\text{O}y}$ scheme (Saiz-Lopez et al., 2014).

Table 3. Iodine chemistry scheme in CAM-Chem: Heterogeneous reactions.

Sea-salt aerosol reactions	Reactive uptake
$\text{IONO}_2 \rightarrow 0.5 \text{ IBr} + 0.5 \text{ ICl}$	$\gamma = 0.01$
$\text{INO}_2 \rightarrow 0.5 \text{ IBr} + 0.5 \text{ ICl}$	$\gamma = 0.02$
$\text{HOI} \rightarrow 0.5 \text{ IBr} + 0.5 \text{ ICl}$	$\gamma = 0.06$
$\text{I}_2\text{O}_2 \rightarrow$	$\gamma = 0.01^{\S}$
$\text{I}_2\text{O}_3 \rightarrow$	$\gamma = 0.01^{\S}$
$\text{I}_2\text{O}_4 \rightarrow$	$\gamma = 0.01^{\S}$

Values based on the THAMO model (Saiz-Lopez et al., 2008) and implemented in CAM-Chem following (Ordóñez et al., 2012).

[§] Deposition of I_xO_y species on sea-salt aerosols has been included following the free regime approximation.

Table 4. Iodine chemistry scheme in CAM-Chem: Henry's Law constants and dry deposition velocities.

Species	k_0 (M atm ⁻¹)	Deposition velocity [§] (cm s ⁻¹)	Reference
IBr ^{ice}	2.4×10^1	–	1
ICl ^{ice}	1.1×10^2	–	1
HI	7.8×10^{-1}	1.0	1 ^a
HOI – ($J_{I_xO_y} / Base$)	$1.9 \times 10^3 / 4.5 \times 10^3$	0.75	1 ^b
IONO ₂ ^{ice}	1.0×10^6	0.75	2 ^c
INO ₂ ^{ice}	3.0×10^{-1}	0.75	1 ^d
IO	4.5×10^2	–	2
OIO	1.0×10^4	–	2
I ₂ O ₂	1.0×10^4	1.0	2
I ₂ O ₃	1.0×10^4	1.0	2
I ₂ O ₄	1.0×10^4	1.0	2

[§] Dry deposition velocities are based on the THAMO model (Saiz-Lopez et al., 2008).

¹ Values reported in (Sander, 1999).

² Values based on the THAMO model (Saiz-Lopez et al., 2008).

^a Considering a dissociation constant $K_a = 3.2 \times 10^9$ and a temperature dependent coefficient $c = 9800$ K

^b Within the range of values given in the corresponding reference.

^c Virtually infinite solubility is represented by using a very large arbitrary number.

^d Value assumed to be equal to those of BrNO₂.

^{ice} Species for which ice-uptake is considered following (Neu and Prather, 2012).

References

Allan, B. J., and Plane, J. M. C.: A Study of the Recombination of IO with NO₂ and the Stability of INO₃: Implications for the Atmospheric Chemistry of Iodine, *J. Phys. Chem. A*, 106, 8634-8641, 2002.

Atkinson, R., Baulch, D. L., Cox, R. A., Crowley, J. N., Hampson, R. F., Hynes, R. G., Jenkin, M. E., Rossi, M. J., and Troe, J.: Evaluated kinetic and photochemical data for atmospheric chemistry: Volume III: gas phase reactions of inorganic halogens, *Atmos. Chem. Phys.*, 7, 981-1191, 2007.

Atkinson, R., Baulch, D. L., Cox, R. A., Crowley, J. N., Hampson, R. F., Hynes, R. G., Jenkin, M. E., Rossi, M. J., Troe, J., and Wallington, T. J.: Evaluated kinetic and photochemical data for atmospheric chemistry: Volume IV – gas phase reactions of organic halogen species, *Atmos. Chem. Phys.*, 8, 4141-4496, 10.5194/acp-8-4141-2008, 2008.

- Bale, C. S. E., Canosa-Mas, C. E., Shallcross, D. E., and Wayne, R. P.: A discharge-flow study of the kinetics of the reactions of IO with CH_3O_2 and CF_3O_2 , *Phys. Chem. Chem. Phys.*, 7, 2164-2172, 2005.
- Bedjanian, Y., Le Bras, G., and Poulet, G.: Kinetic study of the $\text{Br} + \text{IO}$, $\text{I} + \text{BrO}$ and $\text{Br} + \text{I}_2$ reactions. Heat of formation of the BrO radical, *Chem. Phys. Lett.*, 266, 233-238, doi: 10.1016/S0009-2614(97)01530-3, 1997.
- Bösch, H., Camy-Peyret, C., Chipperfield, M. P., Fitzenberger, R., Harder, H., Platt, U., and Pfeilsticker, K.: Upper limits of stratospheric IO and OIO inferred from center-to-limb-darkening-corrected balloon-borne solar occultation visible spectra: Implications for total gaseous iodine and stratospheric ozone, *J. Geophys. Res.*, 108, 4455, 2003.
- Chambers, R. M., Heard, A. C., and Wayne, R. P.: Inorganic gas-phase reactions of the nitrate radical: iodine + nitrate radical and iodine atom + nitrate radical, *J. Phys. Chem.*, 96, 3321-3331, 10.1021/j100187a028, 1992.
- Chameides, W. L., and Davis, D.: Iodine: Its Possible Role in Tropospheric Photochemistry, *J. Geophys. Res.*, 85, 7383-7398, 1980.
- Dillon, T. J., Karunanandan, R., and Crowley, J. N.: The reaction of IO with CH_3SCH_3 : products and temperature dependent rate coefficients by laser induced fluorescence, *Phys. Chem. Chem. Phys.*, 8, 847-855, 2006a.
- Dillon, T. J., Tucceri, M. E., and Crowley, J. N.: Laser induced fluorescence studies of iodine oxide chemistry Part II. The reactions of IO with CH_3O_2 , CF_3O_2 and O_3 ., *Phys. Chem. Chem. Phys.*, 8, 5185-5198, 2006b.
- Dillon, T. J., Tucceri, M. E., Sander, R., and Crowley, J. N.: LIF studies of iodine oxide chemistry Part 3. Reactions $\text{IO} + \text{NO}_3 \rightarrow \text{OIO} + \text{NO}_2$, $\text{I} + \text{NO}_3 \rightarrow \text{IO} + \text{NO}_2$, and $\text{CH}_2\text{I} + \text{O}_2 \rightarrow$ (products): implications for the chemistry of the marine atmosphere at night., *Phys. Chem. Chem. Phys.*, 10, 1540-1554, 2008.
- Dooley, K. S., Geidosch, J. N., and North, S. W.: Ion imaging study of IO radical photodissociation: Accurate bond dissociation energy determination, *Chem. Phys. Lett.*, 457, 303-306, 2008.
- Drougas, E., and Kosmas, A. M.: Ab Initio Characterization of (CH_3IO_3) Isomers and the $\text{CH}_3\text{O}_2 + \text{IO}$ Reaction Pathways, *J. Phys. Chem. A*, 111, 3402-3408, 2007.
- Enami, S., Yamanaka, T., Hashimoto, S., Kawasaki, M., Nakano, Y., and Ishiwata, T.: Kinetic Study of IO Radical with RO_2 ($\text{R} = \text{CH}_3$, C_2H_5 , and CF_3) Using Cavity Ring-Down Spectroscopy, *J. Phys. Chem. A*, 110, 9861-9866, 2006.
- Galvez, O., Gomez Martin, J. C., Gomez, P. C., Saiz-Lopez, A., and Pacios, L. F.: A theoretical study on the formation of iodine oxide aggregates and monohydrates, *Phys. Chem. Chem. Phys.*, 15, 15572-15583, 10.1039/C3CP51219C, 2013.
- Gilles, M. K., Turnipseed, A. A., Burkholder, J. B., and Ravishankara, A. R.: A study of the $\text{Br} + \text{IO} \rightarrow \text{I} + \text{BrO}$ and the reverse reaction, *Chem. Phys. Lett.*, 272, 75-82, doi: 10.1016/S0009-2614(97)00485-5, 1997.
- Glowacki, D. R., Liang, C.-H., Morley, C., Pilling, M. J., and Robertson, S. H.: MESMER: An Open-Source Master Equation Solver for Multi-Energy Well Reactions, *J. Phys. Chem. A*, 116, 9545-9560, 10.1021/jp3051033, 2012.
- Gómez Martín, J. C., Spietz, P., and Burrows, J. P.: Kinetic and Mechanistic Studies of the I_2/O_3 Photochemistry, *J. Phys. Chem. A*, 111, 306-320, 2007.

Gómez Martín, J. C., and Plane, J. M. C.: Determination of the O-IO bond dissociation energy by photofragment excitation spectroscopy, *Chem. Phys. Lett.*, 474, 79-83, 2009.

Jenkin, M. E., Cox, R. A., and Candeland, D. E.: Photochemical Aspects of Tropospheric Iodine Behavior, *J. Atmos. Chem.*, 2, 359-375, 1985.

Kaltsoyannis, N., and Plane, J. M. C.: Quantum chemical calculations on a selection of iodine-containing species (IO, OIO, INO_3 , $(\text{IO})_2$, I_2O_3 , I_2O_4 and I_2O_5) of importance in the atmosphere., *Phys. Chem. Chem. Phys.*, 10, 1723-1733, 2008.

Knyazev, V. D., and Slagle, I. R.: Thermochemistry of the R-O2 Bond in Alkyl and Chloroalkyl Peroxy Radicals, *J. Phys. Chem. A*, 102, 1770-1778, 10.1021/jp9726091, 1998.

Lancar, I. T., Mellouki, A., and Poulet, G.: Kinetics of the reactions of hydrogen iodide with hydroxyl and nitrate radicals, *Chem. Phys. Lett.*, 177, 554-558, 1991.

Laszlo, B., Huie, R. E., Kurylo, M. J., and Miziolek, A. W.: Kinetic studies of the reactions of BrO and IO radicals, *J. Geophys. Res.*, 102, 1997.

McFiggans, G., Plane, J. M. C., Allan, B. J., Carpenter, L. J., Coe, H., and O'Dowd, C.: A modeling study of iodine chemistry in the marine boundary layer, *J. Geophys. Res.*, [Atmos.], 105, 14371-14385, 2000.

Neu, J. L., and Prather, M. J.: Toward a more physical representation of precipitation scavenging in global chemistry models: cloud overlap and ice physics and their impact on tropospheric ozone, *Atmos. Chem. Phys.*, 12, 3289-3310, 10.5194/acp-12-3289-2012, 2012.

Ordóñez, C., Lamarque, J. F., Tilmes, S., Kinnison, D. E., Atlas, E. L., Blake, D. R., Sousa Santos, G., Brasseur, G., and Saiz-Lopez, A.: Bromine and iodine chemistry in a global chemistry-climate model: description and evaluation of very short-lived oceanic sources, *Atmos. Chem. Phys.*, 12, 1423-1447, 10.5194/acp-12-1423-2012, 2012.

Plane, J. M. C., Joseph, D. M., Allan, B. J., Ashworth, S. H., and Francisco, J. S.: An Experimental and Theoretical Study of the Reactions $\text{OIO} + \text{NO}$ and $\text{OIO} + \text{OH}$, *J. Phys. Chem. A*, 110, 93-100, 2006.

Saiz-Lopez, A., Plane, J. M. C., Mahajan, A. S., Anderson, P. S., Bauguitte, S. J.-B., Jones, A. E., Roscoe, H. K., Salmon, R. A., Bloss, W. J., Lee, J. D., and Heard, D. E.: On the vertical distribution of boundary layer halogens over coastal Antarctica: implications for O_3 , HO_x , NO_x and the Hg lifetime, *Atmos. Chem. Phys.*, 8, 887-900, 2008.

Saiz-Lopez, A., Fernandez, R. P., Ordóñez, C., Kinnison, D. E., Gómez Martín, J. C., Lamarque, J. F., and Tilmes, S.: Iodine chemistry in the troposphere and its effect on ozone, *Atmos. Chem. Phys.*, 14, 13119-13143, 10.5194/acp-14-13119-2014, 2014.

Sander, R.: Compilation of Henry's Law Constants for Inorganic and Organic Species of Potential Importance in Environmental Chemistry (v3), available at: <http://www.henrys-law.org/> (last access: 1 Sept 2016), 1999.

Sander, S. P., Friedl, R. R., Golden, D. M., Kurylo, M. J., Moortgat, G. K., Wine, P. H., Ravishankara, A. R., Kolb, C. E., Molina, M. J., Diego, S., Jolla, L., Huie, R. E., and Orkin, V. L.: Chemical Kinetics and Photochemical Data for Use in Atmospheric Studies Evaluation Number 15, JPL_NASA, 06-2, Jet Propulsion Laboratory, Pasadena, CA, 2006.

Sander, S. P., Friedl, R. R., Barker, J. R., Golden, D. M., Kurylo, M. J., Sciences, G. E., Wine, P. H., Abbatt, J. P. D., Burkholder, J. B., Kolb, C. E., Moortgat, G. K., Huie, R. E., and Orkin, V. L.: Chemical Kinetics and Photochemical Data for Use in Atmospheric Studies, Evaluation No. 17, JPL_NASA, 10-6, Jet Propulsion Laboratory, Pasadena, CA, 2011.